

Long-Term Volumetric Eruption Rates and Magma Budgets

Scott M. White
Dept. Geological Sciences
University of South Carolina
Columbia, SC 29208
swhite@geol.sc.edu

Joy A. Crisp
Jet Propulsion Laboratory, California Institute of Technology
Pasadena, CA 91109
Joy.A.Crisp@jpl.nasa.gov

Frank J. Spera
Dept. Earth Science
University of California, Santa Barbara
Santa Barbara, CA 93106
spera@geol.ucsb.edu

Corresponding Author:

Scott White
Dept. of Geological Sciences
700 Sumter Street
University of South Carolina
Columbia, SC 29208
Tel: (803) 777-6304, Fax: (803) 777-6610

Abstract

A global compilation of 170 time-averaged volumetric volcanic output rates (Q_e) are evaluated in terms of composition and petrotectonic setting to advance the understanding of long-term rates of magma generation and eruption on Earth. Repose period between successive eruptions at a given site and intrusive:extrusive ratios were compiled for selected volcanic centers where long-term ($>10^4$ a) data were available. More silicic compositions, rhyolites and andesites, have a more limited range of eruption rates than basalts. Even when high Q_e values contributed by flood basalts ($9\pm 2\times 10^{-1}$ km³/a) are removed, there is a trend in decreasing average Q_e with lava composition from basaltic eruptions ($2.6\pm 1.0\times 10^{-2}$ km³/a) to andesites ($2.3\pm 0.8\times 10^{-3}$ km³/a) and rhyolites ($4.0\pm 1.4\times 10^{-3}$ km³/a). This trend is also seen in the difference between oceanic and continental settings, as eruptions on oceanic crust tend to be predominately basaltic. All of the volcanoes occurring in oceanic settings fail to have statistically different mean Q_e and have an overall average of $2.8\pm 0.4\times 10^{-2}$ km³/a, excluding flood basalts. Likewise, all of the volcanoes on continental crust fail also fail to have statistically different mean Q_e and have an overall average of $4.4\pm 0.5\times 10^{-3}$ km³/a. Flood basalts also form a distinctive class with an average Q_e higher nearly two orders of magnitude higher than any other class. However, we have found no systematic evidence linking increased intrusive:extrusive ratios with lower volcanic rates. A simple heat balance analysis suggests that the preponderance of volcanic systems must be open magmatic systems with respect to heat and matter transport in order to maintain eruptible magma at shallow depth throughout the observed lifetime of the volcano. The empirical upper limit of circa 10^{-2} km³/a for magma eruption rate in systems with relatively high intrusive:extrusive ratios may be a consequence of the fundamental parameters governing rates of melt generation (e.g., subsolidus isentropic decompression, hydration due to slab dehydration and heat transfer between underplated magma and the overlying crust) in the Earth.

1. Introduction

Despite the significant impact of volcanic systems on climate, geochemical cycles, geothermal resources and the evolution and heat budget of the crust, surprisingly little is known regarding the systematics of long-term rates of magma generation and eruption on Earth. Global rates of magma generation provide insight regarding the planetary-scale energy budget and thermal evolution of the Earth. Rates of magma generation and eruption are key factors affecting the petrological and geochemical evolution of magma bodies as well as eruptive styles due to the intrinsic coupling between magma recharge, fractional crystallization, wall rock assimilation and melt volatile saturation [Shaw, 1985; Spera *et al.*, 1982]. Volcanoes and formation of intrusive bodies such as sill complexes have been suggested to play a role in global climate change [Svensen *et al.*, 2004] and perhaps even trigger biotic extinctions. In addition, global rates of magmatism may have important implications for seismic energy release [Shaw, 1980] and the magnetic geodynamo by modulating heat transfer from the core-mantle boundary and the concomitant development of deep mantle plumes [Olson, 1994]. Rates of magmatism on Earth are also used in planetary research as analogues to constrain magmatic and thermal models. In summary, there is an exhaustive set of reasons for developing systematic knowledge regarding the rates of magmatism on Earth including the effects of magma composition and prototectonic environment on volumetric rates.

One of the key factors in understanding magmatism is a quantitative evaluation of the extent to which magmatic systems operate as open or closed systems. These alternatives have significantly different implications for magma evolution. However, the openness of magmatic systems is difficult to determine since there is no unambiguous way to track magma transport from the generation and segregation through the crust to volcanic output. On balance, many magma systems are thought to be open systems in that they receive additional inputs of heat and mass during magmatic evolution [Davidson *et al.*, 1988; Fowler *et al.*, 2004; Gamble *et al.*, 1999; Hildreth *et al.*, 1986; Petford and Gallagher, 2001]. Closed magmatic systems which exchange heat but little material with their surroundings (i.e., neither assimilation nor recharge is important) may be rather uncommon. What is more likely is that specific systems may behave as closed systems for restricted portions of their history (e.g., [Singer *et al.*, 1992; Zielinski and Frey, 1970]). It is important to note, however, for the olivine basalt-trachyte series at Gough Island where fractional crystallization appears dominant, Pb and Sr isotopic data indicate that assimilation of hydrothermally-altered country rock and or recharge of isotopically distinct magma has taken place [Oversby and Gast, 1970].

In this paper, time-averaged volcanic output for periods $>10^3$ years are evaluated. Volcanic output rates for individual eruptions may vary wildly about some norm, but evidently settle to a representative “average” value when time windows on the order of 10 times the average interval of eruptions are considered [Wadge, 1982]. Crisp [1984] conducted a similar study of magmatic rates published between 1962-1982 and established some basic relationships between volcanic output and associated factors such as crustal thickness, magma composition, and prototectonic setting. This work updates and extends that earlier compilation with 98 newly published volcanic rates and volumes

from 1982-2004 for a total of 170 estimates. We also endeavor to establish some scaling relationships based primarily on the compilation and some simple energy budget considerations with the goal of discovering possible systematic trends in the data.

1.1. Sources and Quality of the Data

The data presented here are volumetric volcanic or intrusive rates published from 1962-2005, including data from the compilation by Crisp [1984] of rates published from 1962-1982 where these data have not been superseded by more recent studies. We have also reviewed the rate data presented in Crisp [1984] and corrected or removed several references as appropriate. Thus, the data presented here is a completely updated compilation of volumetric rates of eruption.

Most volcanoes have cycles of intense activity followed by repose. Comparing volcanic systems at different stages in their eruptive cycles can lead to erroneous conclusions, if the duration of activity is not long enough to average the full range of eruptive behavior over the lifetime of the volcano. The duration needed depends upon the individual volcano; longer periods are generally required for volcanic centers erupting more compositionally-evolved magma due to lower eruption recurrence interval. Thus, a period of $\sim 10^3$ years may be a long time for a basaltic shield volcano (e.g., Kilauea, Hawaii) but captures only an insignificant fraction of one eruptive cycle at a rhyolitic caldera (e.g., Yellowstone, USA). Only long-term rates are considered in this study although this reduces the available data considerably. We have culled the data to include primarily those estimates over 10^4 years or longer, but have selected a few volcanic centers with shorter durations where the shorter time interval did not compromise the data quality (e.g. capturing several eruptive cycles, smaller volcanic centers, or similar reasons) in our judgment.

Tables 1 and 2 show volcanic output rates for primarily mafic and silicic systems respectively. Output rates for volcanic systems (Q_e) are determined by dividing volcanic output volume by the duration of the activity. For longer durations activity may not have been continuous. By use of density for different compositions [Spera, 2000] we can convert volume rate (Q_e) to mass rate, which is probably the more fundamental parameter. Since density varies only slightly (basalt is $\sim 15\%$ denser than rhyolite at the same temperature and pressure) compared to the uncertainty in the data and the original data are all reported in terms of volume, we use Q_e exclusively in the rest of this study although mass rates are also given in Tables 1 and 2. Within each table, the rate estimates encompassing large areas, such as entire arcs or extensive volcanic fields, are presented separately from rates for individual volcanoes or smaller fields of vents. To remove ambiguity from the decision, a cutoff of 10^4 km² was used to separate global datasets, typically involving compilations of several volcanoes themselves, from local datasets focused on individual volcanoes with a more constrained study area. However, we find that rates for entire arcs when presented as km³/a per 100 km arc length are similar to those for individual volcanoes (Figure 1).

A large amount of uncertainty is associated with inferring volcanic rates from unobserved eruptions. In the tables, a “Notes” field contains information about the methods used to derive the estimates and uncertainties that were available in the original literature, but in many cases no formal uncertainties were reported. Generally the rates reported here

should be taken as order-of-magnitude estimates although in some cases the uncertainties may be as small as a factor of two. The extrusive rate often depends on the duration considered; therefore data for one volcanic center measured over different durations is included in Tables 1 and 2. The period of volcanism may also be important since eruptions from farther in the past may have experienced more erosion, partial burial, or be more difficult to accurately date.

Sources of error reported in the original publications, as well as most unquantified unreported error, mainly arise from estimating (1) the thickness of the volcanic deposits, (2) the age of volcanic deposits, or (3) amount of erosion. Less significant potential sources of error are uncertainty in the conversion from volume to dense rock equivalent (DRE) volume, and uncertainty in the area covered by deposits. One may attribute some of the variance in rates to error introduced by comparing volcanic systems at different scales. For example, the volcanic output rate over continuous lengths of oceanic arcs and ridges is expected to be higher than small individual volcanoes. The arcs and ridges are divided into unit volcano lengths of 100 km based on the spacing of volcanoes in arcs [*de Bremond d'Ars et al.*, 1995]. Petrologic and tectonic factors reported for each volcanic system where data are available include lithic type or bulk wt % SiO₂ of erupted magma, and petrotectonic setting. Rock names are given for the dominant magma type associated with each area simplified in one of the following categories: basalt, basaltic andesite, andesite, rhyolite. The mode wt % SiO₂ reported here is the mode of erupted products by volume reported within the given period for that volcanic system. Petrotectonic setting groups the systems into six categories based on crustal type, oceanic or continental, and association with a plate boundary type; convergent, divergent, or intraplate.

2. Volcanic Rates and Regimes

2.1. Rates of Eruption

Eruption rates are examined on the basis of dominant lithology and petrotectonic setting. Rock type affects many factors related to flow behavior such as viscosity, temperature, and pre-eruptive volatile content. Thus, it may be an important control on eruption rate. Petrotectonic setting most strongly reflects the magma generation process, but is also a way to qualitatively look at the effects of crustal thickness.

The effect of magma composition on eruption rate is assessed by broadly grouping the volcanic deposits from an area into one of four categories based on the dominant SiO₂ of the reported rock compositions: basalt, basaltic andesite, andesite, or rhyolite. Many important physical properties of magma are a function of SiO₂ content, as well as being easy to measure and widely reported, making this a useful tool for first-order comparison of volcanoes. The rock type dominant in the area is assigned as the rock type to represent the entire area. For example, Yellowstone is assigned as rhyolite on the basis of its repeated large caldera-forming eruptions even though a small amount of basalt leaks out between large-volume paroxysmal rhyolite eruptions. Where bimodal volcanism is equally balanced by volume or a change in rock type has occurred at some point in the eruptive history of the volcanic system, the basaltic (Table 1) and silicic (Table 2) volumes and rates of eruption are reported separately. For example, recent Kamchatka eruptions are split into andesites (Table 2) and basalts (Table 1).

Basalts exhibit a wider range of eruption rates than other rock types, ranging from $<10^{-5}$ km^3/a to >1 km^3/a (Figure 1). Basaltic systems in general show both short-term and long-term changes in eruption rates especially in long-lived systems (e.g. Hawaii, [Dvorak and Dzurisin, 1993; Vidal and Bonneville, 2004]). More-silicic rock types, the rhyolites and andesites, have a more limited range of eruption rates than basalts. Long-term rates for silicic eruptions range from $<10^{-5}$ km^3/ka to 10^{-2} km^3/a (Table 2 and Fig. 1). Among the major rock type groups we have used here, the mean and variance of Q_e decreases as the amount of silica increases. In Figure 1, this trend is apparent as the basalts form a wide field of values whose mean is 10^{-2} km^3/a while andesites and rhyolites form a much narrower band of values around 10^{-3} km^3/a . The flood basalts form a small cluster of values above 1 km^3/a on Figure 1, outside of a more uniform field of values for all compositions, and seem to form a distinct group. Therefore, flood basalts were not considered with the rest of the basalt rates when comparing to other compositions to avoid skewing the results. With flood basalts removed, basaltic eruptions still have an order-of-magnitude higher average rate ($2.6 \pm 1.0 \times 10^{-2}$ km^3/a) than basaltic andesites, andesites and rhyolites. Average rates for andesites ($2.3 \pm 0.8 \times 10^{-3}$ km^3/a) and rhyolites ($4.0 \pm 1.4 \times 10^{-3}$ km^3/a) are also significantly different, although not as distinct as the difference between basalts and these two groups.

The effect of petrotectonic setting on eruption rate is assessed by grouping the volcanoes by the main differences in magma genesis based on plate tectonic theory. In contrast to lithology, petrotectonic setting lends itself to grouping into categories (Figure 2). Volcanoes at convergent plate boundaries are arcs, divergent plate boundaries are rifts or spreading ridges, and intraplate volcanoes are so-called hotspots. Also included is a separate designation of volcanic fields for areas characterized by areally distributed volcanism of primarily small (<1 km^3), monogenetic cones. These fields tend to occur in regions that are difficult to classify by traditional plate tectonic theory such as slab windows (e.g., Clear Lake, CA) or continental extension (e.g., Lunar Crater, NV). In order to also assess the role of crustal thickness/composition, the petrotectonic settings are further subdivided into volcanoes erupting through continental or oceanic crust. The exceptions are oceanic plateaux, the flood basalt equivalent for oceanic crust. Reliable data are so sparse for plateaux that we have grouped oceanic and continental flood basalts in Figure 2.

Flood basalts have the highest single Q_e value and mean Q_e of any volcanic system on Earth (Figure 2). In this respect, flood basalts form an exceptional group unlike the other forms of terrestrial volcanism. In contrast, the continental volcanic fields have the lowest single and mean Q_e of any group. A very wide range of eruption rates have been reported for oceanic hotspots that overlaps significantly with oceanic arcs and ocean spreading ridges. Although the mean Q_e appears higher for oceanic hotspots than other classes of oceanic volcanism, the two-tailed t-test indicates that Q_e for all groups of oceanic volcanism are not statistically different. When grouped by petrotectonic setting, Q_e from continental areas stand out as being lower on average than for oceanic areas, however the range of output rates for any one setting overlaps all other settings (Fig. 2). Crisp [1984] noted a similar pattern of higher eruption rates in oceanic settings although found no specific value of crustal thickness that acted as a filter threshold. All of the volcanoes occurring in oceanic settings fail to have statistically different mean Q_e and have an

overall average of $2.8 \pm 0.8 \times 10^{-2} \text{ km}^3/\text{a}$. Likewise, all of the volcanoes on continental crust also fail to have statistically different mean Q_e and have an overall average of $4.4 \pm 0.5 \times 10^{-3} \text{ km}^3/\text{a}$, excluding flood basalts. A two-tailed t-test for means indicates that oceanic and continental Q_e are statistically different. Flood basalts also form a distinctive class of volcanism with an average Q_e ($9 \pm 2 \times 10^{-1} \text{ km}^3/\text{a}$) two orders of magnitude larger than the range of any other class (Figure 2).

2.2. Intrusive:Extrusive Ratios

The average and range of intrusive:extrusive (I:E) volume ratios for different petrotectonic settings are useful in estimating hidden intrusive volumes at other locations and perhaps on other planets [Greeley and Schneid, 1991]. However, I:E ratios are difficult to estimate and rarely published because the plutonic rocks are either buried or the volcanic rocks are eroded, or the relationship between the volcanic and plutonic rocks is uncertain. Seismic, geodetic, and electromagnetic techniques can reveal the dimensions of molten or partially molten regions under a volcano. Likewise, the sulfur output by magma degassing can be used to estimate the volume of the cooling magma [Allard, 1997]. However, the size of the molten magma reservoir at one time in a longer history may not be a good indicator of the total intrusive volume. Likewise, broad constraints on intrusive volume based on petrologic modeling of the fractional crystallization of a parent basalt are not considered because they will always calculate lower bound on intrusive volume, because such calculations cannot account for strictly intrusive events. Better estimates of total intrusive volume can sometimes be obtained by seismic or gravity measurements of buried plutons. Another way to determine I:E ratios is to compare geographically related volcanic and plutonic sequences. Three such determinations were made in this compilation for the Andes, the Bushveld Complex, and the Challis Volcanic Field-Casto Pluton. However, in each of these cases it is uncertain how well linked extrusive and intrusive rocks are in fact. Despite this uncertainty, we proceed with an analysis if for no other reason than to highlight that this issue has received so little attention.

Previous studies have reported a wide range of I:E ratios from 1:1 to 16:1 [Crisp, 1984; Shaw *et al.*, 1980; Wadge, 1980]. Shaw [1980] hypothesized that the I:E ratio would be higher where crustal thickness is greater, up to 10:1. This makes sense since magma traveling greater path lengths through thicker continental crust has longer to cool and dissipate energy. In addition, mean crustal densities are closer to typical magma densities compared to the mantle (i.e., positive buoyancy forces are likely smaller for magma in the crust compared to magma in the mantle). Subsequently, Wadge [1982] made the argument based on steady-state volcanic rates and indirect calculations of intrusive volume that less evolved systems have I:E ratios as low as 1:1.5 for basaltic shields on oceanic crust and up to 1:10 for rhyolite calderas on continental crust. Crisp [1984] presented 14 ratios but did not find any strong connection between magma composition and I:E ratio.

The I:E ratios in this compilation encompass a wide range of values but fails to show any systematic variations with eruptive style, volcanic setting, or total volume (Table 3). While some well known basaltic shields do have I:E ratios of 1:1 to 2:1, the oceanic ridges have considerably higher ratios of at least 5:1. The range of estimates goes as high

as 34:1 at Mount Pinatubo, and 200:1 for the Coso Volcanic Field. Conversely, the I:E ratios at calderas may be much lower than 10:1. Yellowstone has a fairly well constrained I:E ratio of 3:1. Continental magma systems that have had detailed geophysical investigations tend to have magma chamber volume estimates comparable to the total erupted volume, as noted by Marsh [1989]. A ratio of 5:1 could be viewed as common to most magmatic systems when the considerable uncertainty is considered. Ratios higher than 10:1 are uncommon in our dataset. When volume of magma involved in crustal “underplating” or magmatic addition to the lower crust is also counted, much higher ratios of intrusive:extrusive activity sometimes result (Ninetyeast Ridge [Frey *et al.*, 2000], Coso [Bacon *et al.*, 1983]) but other times do not (Aleutians [Kay and Kay, 1985], Marquesas [Caress *et al.*, 1995]).

2.3. Repose Time between Volcanic Events

A major discriminant in the behavior of volcanic systems is their frequency of eruptions through time. Most basaltic volcanoes erupt small volumes of lava frequently whereas continental calderas erupt great volumes of silicic magma infrequently. At Hekla, Thorarinsson and Sigvaldason {, 1972 #385} noted a positive relationship between repose length and the silica content of the initial lavas erupted following the repose. Data from 17 volcanic centers in Table 4 selected to span a wide range of SiO₂ content define an exponential relationship between repose time and SiO₂ content of the magma (Figure 3). The volcanic centers in Table 4 were chosen to span a range of SiO₂ compositions for sequences of at least three eruptions.

The minimum, maximum, and mean repose time for an eruption sequence is presented along with the minimum and maximum SiO₂ content for the corresponding suite of compositions erupted from a ‘single’ center. Repose time is determined by the interval between the end of one eruption and the start of the next. Measuring repose time is somewhat subjective because what may count as a repose at one volcano may not be considered as a repose elsewhere. Closely observed volcanoes (e.g. Etna or Kilauea) have repose reported on a scale of days but older or more silicic volcanoes (e.g. Santorini or St. Helens) have their eruptive periods divided into major eruptive units separated by thousands of years. We have tried to determine repose period as the length of time between eruptions of a characteristic size for that volcano. For example, at Santorini repose between the Kameni dome-forming eruptions are much shorter than the major ashfall eruptions [Druitt *et al.*, 1999]. This example also highlights the potential for bias toward the Recent with shorter repose times for smaller eruptions that are not preserved in the long-term geologic record. For these reasons, the repose between major eruptions are considered whereas the “leaking” of minor volumes of lava between major eruptions is not considered in this study.

The exponential relationship between SiO₂ content and repose time is mainly determined by basaltic shields and rhyolite calderas. For volcanoes in the andesite-dacite range, the data jump from short repose intervals to longer repose at ~60% SiO₂ (Figure 3). While composition is unlikely to be the exclusive control on repose time, more error is likely to emerge in the 60-70% SiO₂ range due to difficulties in dating the eruptions of complex stratocones, the dominant constructional volcanic morphology for intermediate compositions. Measuring the repose periods at stratocones and calderas requires high

resolution stratigraphy and precise ages over several millennia to smooth out the short-timescale volume/frequency relationship [Wadge, 1982]. These data are very limited but are becoming more available recently with improvements in geochronological methods [Hildreth *et al.*, 2003a]. If the maximum SiO₂ in the system controls the repose period then the fit parameter of the exponential equation improves slightly ($R^2=0.69$ to 0.73).

There are several reasons to expect repose time to increase as silica increases. Direct melting of mantle produces basaltic compositions, and more evolved compositions require time for fractional crystallization and assimilation. Higher silica compositions also have greater melt viscosity, requiring additional excess pressure to erupt [Rubin, 1995] and, in that sense, are far less mobile. More viscous magmas are more likely to suffer ‘thermal death’ compared to less viscous magmas. A few studies have already pointed out a positive correlation between eruptive volume and repose interval [Cary *et al.*, 1995; Klein, 1982; Wadge, 1982]. The magma storage time, based on rock geochronometers from crystal ages and from crystal size distribution analysis (CSD), tends to increase exponentially as SiO₂ and stored magma volume increase [Hawkesworth *et al.*, 2004; Reid, 2003]. These observations are all consistent with the idea that longer magma storage times allow more time for fractional crystallization and assimilation, in turn, results in longer repose periods associated with higher silica content magmas.

3. Discussion

3.1. Upwelling and Magma Production Rate Limits

Factors that might influence volcanic rates and intrusive:extrusive ratios are local crustal thickness, tectonic setting (magnitude and orientation of principal stresses), magma composition, and melt generation rate in the source region. For 160 examples, long-term volcanic output rate varies from 10^{-5} to $1 \text{ km}^3/\text{a}$. Only flood basalts attain the highest Q_e , above $10^{-1} \text{ km}^3/\text{a}$, while various volcanoes with the lowest measured Q_e , below $10^{-5} \text{ km}^3/\text{a}$, seem to have very little in common (Figure 1). Tectonic setting, but not magma composition, affects volcanic rates. Continental crust reduces the average Q_e to $5 \times 10^{-3} \text{ km}^3/\text{a}$ from 4×10^{-1} for oceanic crust, but the two volcano populations have a large range of overlap.

The output rates all show a strong skewness with long tails toward low Q_e values suggesting that an upper limit may exist (Figure 2). Furthermore, although there is essentially no lower limit to volcanic rates in that magma supplied from depth may intrude but never erupt, or dribble out slowly, this is not usually the case. Most volcanoes have a Q_e above $1 \times 10^{-3} \text{ km}^3/\text{a}$. This result was also found empirically by Smith [1979] and Crisp [1984]. Hardee [1982] derives a simple analytic solution showing that this critical Q_e of $\sim 10^{-3} \text{ km}^3/\text{a}$ represents a ‘thermal threshold’ where magmatic heat from the intrusion tends to keep a conduit open and begin formation of a magma chamber. We infer that long-term volcanism is unlikely to occur without an open magma conduit to supply and focused melt delivery. This threshold value is dependent on intrusive rate, not volcanic output rate. The I:E ratios found are somewhat lower than the often cited 10:1 ratio, and suggest that an I:E ratio of $\sim 5:1$ may be regarded as a better average value. Nevertheless, this suggests that, using the Q_e values present here as data for the Hardee

[1982] model, virtually all of the volcanic systems in Tables 1 and 2 meet the requirements for conduit wall rock meltback and magma chamber formation.

It is perhaps surprising that given the large differences in eruptive style and melt generation mechanisms (e.g., isentropic decompression, triggering by metasomatic introduction of volatiles or mafic magma underplating) in different tectonic settings an aggregate view of volcanic rates exhibits such a small range of variation, by and large. The similarity of the rates leads us to speculate that a magma upwelling rate limit is set within the mantle at a value near $1 \text{ km}^3/\text{a}$, with magma generation being subject to greater variances based on the local composition of the mantle being melted. In this view, flood basalts represent systems with low I:E ratios and form when a large fraction of mantle-generated magma reaches the surface. The upper limit on magma generation may be controlled by the sub-solidus upwelling rate within the upper mantle of $0.01\text{-}0.1 \text{ m/a}$, and this may explain the upper limit of magma generation due to isentropic decompression [Asimow, 2002; Verhoogen, 1954].

3.2. Openness of Magmatic Systems

The volcanic output rate and repose periods between eruptions gives us some basic constraints on the behavior of magma systems as open or closed systems. We have noted the empirical correlation of repose period and magma silica content. That is, a repose interval can be roughly predicted based on either mean or maximum SiO_2 wt % of the eruptive composition. What constraints can be put on storage time in volcanic systems from purely thermodynamic considerations?

A volcanic system can be crudely modeled as a magma storage zone in the crust and a volcanic pile at the surface (Figure 4). Four processes affect the volume of magma in the storage reservoir or magma chamber: eruption (Q_e) and solidification (Q_s) remove magma from the system, while recharge (Q_R) and crustal assimilation (Q_A) add magma to the system. When a volcano acts as a closed system (one that receives no input of mass or heat via advected hot magma) all of the magma erupted remains molten for the duration of volcanic activity under consideration. In such a system, crystallization can occur due to the loss of heat or volatiles from the magma body to its colder surroundings but the extent of crystallization must be insufficient to preclude eruption. One way to approach this problem is to assume that volcanoes act as closed systems during repose periods between eruptions and treat each eruption as the result an isolated batch of magma supplied by recharge in a single event and stored until eruption.

Simple heat transfer considerations based on Stefan cooling of magma permit a first-order test of the hypothesis that a volcanic system is a closed system. If we know the eruption rate (Tables 1 and 2), and assume a closed system with respect to mass and heat recharge, the magma in storage will solidify at a rate specified by Stefan cooling. Using data for volcanic output rate of individual eruptions and repose time between eruptions gathered for several volcanic centers at a wide range of eruptive compositions, a simple 1-D Stefan cooling model [Carslaw and Jaeger, 1959] can be applied to estimate solidification times t (years) in a spherical magma volume of V (km^3)

$$t = \left(\frac{\sqrt[3]{V}}{2\lambda\sqrt{\kappa}} \right)^2 \text{ [EQUATION 1]}$$

where κ is the thermal diffusivity, λ is the solution to the transcendental equation

$$L\sqrt{\frac{\pi}{c_p\Delta T}} = \lambda^{-1} \operatorname{erfc}\lambda e^{-\lambda^2} \text{ [EQUATION 2]}$$

where L is the latent heat of fusion (J kg^{-1}), c_p is the isobaric specific heat capacity ($\text{J kg}^{-1} \text{K}^{-1}$), and ΔT is the temperature difference between the ambient external temperature and the liquidus of the melt phase. The thermal diffusivity is calculated as

$$\kappa = K\rho^{-1}c_p^{-1} \text{ [EQUATION 3]}$$

where ρ is magma density (kg m^{-3}) and K is magma thermal conductivity (J/kg m s). Values for the various constants are taken from Spera [2000] for gabbro, granodiorite, and granite melts. This very basic approach permits a first-order look at the issue of cooling as a constraint on magma system longevity and openness. Heat calculations for lens or sill-like geometries alter the results by a factor of 2-4 [Fedotov, 1982]. Consideration of hydrothermal cooling would tend to enhance cooling rates so that the lifetime of a given volume of magma presented here is always an upper limit on cooling times. A more complex model is not justified given the order-of-magnitude estimates used as input.

If we consider that volcanoes act as closed systems only between two successive eruptions, the solution to the 1D Stefan Problem described above allows us to examine the thermal viability of the volcanic system given the repose period and the volume of magma involved (Figure 5). A closed system, in this context, means that one batch of magma is intruded at some time and stored until the eruption. Thus, a maximum “storage time” for a batch of magma in the shallow plumbing system of a volcano can be estimated (Figure 6). The solidification time is determined as the time for a volume of magma to completely solidify as calculated from equation 1. The volume of magma is assumed to be five times the DRE volume of the eruption following the repose period based on the average I:E ratio from the data in Table 3. The assumption of complete solidification puts an upper limit on the time necessary to cool the magma enough to prevent eruption.

Only a handful of volcanoes have been studied well enough to be able to estimate both volume and timing of eruptions over many eruptive cycles. The long, detailed records of eruptions at Mauna Loa [Klein, 1982] and Etna [Tanguy, 1979; Wadge, 1977] are used as examples of basaltic volcanoes, and the regular eruptive pattern at Izu-Oshima for the past 10^3 years [Koyama and Hayakawa, 1996; Nakamura, 1964] makes the volumes of individual eruptions more clear. Toba [Chesner and Rose, 1991] and Yellowstone [Christiansen, 2001] are two calderas with a high quality record of multiple major eruptions. A few other examples from volcanoes with shorter, but still well documented, records are also used with data from sources cited in Table 2.

Whether the magma would solidify, and thus require the volcano to be an open system, depends on the magma storage time. Estimates of magma storage times from various crystal-age geochronometers are available at a range of volcanic centers and suggest that magma storage period, like repose, is a function of silica content of the magma (see Reid [2003] and refs therein). Storage time from crystal ages for basaltic systems are generally longer or equal to repose, while storage times for andesites and rhyolite systems are slightly shorter than or equal to repose. Based on this information, we can draw a set of lines for different fractions of storage to repose time representing the limits for volcanoes that may be thermally closed systems between eruptions (Fig. 6).

The repose time between eruptions at large calderas (Yellowstone, Long Valley, and Toba) can be more than 10 times greater than the storage time and the volcanoes are still required to be open systems in this analysis (Fig. 6). The basaltic systems (Etna, Mauna Loa, and Oshima) are required to be open systems in this analysis only if magma stored is more than 10-100 times longer than the repose period (Fig. 6). A few outliers for Etna with extremely short eruption repose arguably may be the same eruption, but it is easy to see why these might be from “closed” systems on the timescales presented.

3.3. Heat Flux Associated with Magma Transport

Rates of magmatism may be translated into excess heat flows for specific magmatic provinces to obtain estimates of advected heat via magmatism at regional scales over magmatic province timescales. For mafic eruption rate Q_e and an I:E ratio of \mathfrak{R} , the volumetric rate of magma flow into the crust is $\mathfrak{R}Q_e$. The excess heat power H (J a^{-1}) associated with magma transport from mantle to crust is

$$H = \mathfrak{R} \rho Q_e \Delta T [c_p + L / (T_{\text{liquidus}} - T_{\text{solidus}})] \quad [\text{Equation 4}]$$

where ΔT is the temperature difference between the magma and local crust, L is the enthalpy of crystallization (250-400 kJ/kg dependent on magma composition), ρ is magma density, c_p is the isobaric heat capacity of the magma, and $T_{\text{liquidus}} - T_{\text{solidus}}$ is the liquidus to solidus temperature interval.

As an example, consider the Skye sub-province of the British Tertiary Igneous Province (BTIP). For the estimated volume eruption rate of $2 \times 10^{-3} \text{ km}^3/\text{a}$ averaged over $\sim 1600 \text{ km}^2$ area of Skye, the average excess heat flow is $\sim 3.5 \times 10^7 \text{ J/m}^2/\text{a}$ (1.1 W/m^2). This excess heat flux is more than an order of magnitude greater than the average terrestrial global heat flux 0.09 W m^{-2} . These estimates are consistent with a crustal thickening rate of $\sim 5 \text{ km/My}$ and a background (regional) heat flux of 10-15 times the global average during 60–53 Ma. We conclude that the volume flux of magma in the active years of this part of the BTIP focused heat flow about an order of magnitude above the background at the regional scale for $\sim 5 \text{ Ma}$. The regional energy/mass balance estimate appears consistent with inferences drawn from geochemical modeling that point to significant magma recharge during magmatic evolution at Skye [Fowler *et al.*, 2004].

The excess heat power divided by the area affected by volcanism can be compared to the average terrestrial heat flux to the area. The heat power into the crust due to magmatism is therefore approximately 10^{17} J/a for an overall average eruption rate taken from Table

1 of 10^{-2} km³/a for ~ 1000 km² of arc or ridge and I:E ratio of 5. Thus, typical values for the “average” magmatic system, 10^1 W/m², exceed the global terrestrial background value of 10^{-1} W/m² by two orders of magnitude.

4. Conclusions

The 170 long-term estimates of volcanic output rate compiled from literature references from 1962-2004 corroborate much of the previously published information about magmatic systems but also revealed a few surprises. Long-term volcanic rates are higher for basaltic volcanoes than andesitic and rhyolitic volcanoes taken as a group. Oceanic hotspots, arcs, and ridges have an average volcanic output rate of 10^{-2} km³/a while continental arcs and hotspots have an average output rate of 10^{-3} km³/a, implying that thinner crust/lithosphere is associated with higher volcanic rates on average but not systematically.

For the small number of volcanic systems where adequate data exist (Table 3), the I:E ratio is most commonly less than 10:1 with 2-3:1 being the most commonly occurring value, and a median value of 5:1. Based on the data compiled here, there is little indication that composition is strongly or systematically associated with I:E ratio. We conclude only that further work needs to be done on this important topic.

In contrast, composition and repose period between eruptions (end to next start) are strongly linked. We found that an exponential relationship between repose period and silica content of the magma provides a satisfactory fit to the data.

Based purely on thermal considerations, volcanic systems must be open to recharge of magma between individual eruptions, except for the most frequently erupting basaltic volcanoes. The fact that basaltic systems are indeed open magmatic systems can be demonstrated by other means (e.g. [Davidson *et al.*, 1988; Gamble *et al.*, 1999; Hildreth *et al.*, 1986]).

Acknowledgements

The authors would like to thank Arwen Vidal, Yanhua Anderson, and Joseph Goings for tracking down some of the data that went into the tables. Some of the work that went into this paper was carried out at and for the Jet Propulsion Laboratory, California Institute of Technology, sponsored by the National Aeronautics and Space Administration. Support from NASA, NSF and the DOE for magma transport research at UCSB is gratefully acknowledged. We thank M. R. Reid, C. R. Bacon, and R. S. J. Sparks for their very thorough and thoughtful reviews.

Figure Captions

Figure 1: Volumes and volcanism durations for locations in Tables 1 and 2. The diagonal lines represent constant rates of volcanic output. The points are color coded to indicate lava composition by SiO₂ content. Circles represent rates for arc and large areas ($>10^4$ km²) and crosses represent individual volcanoes and small volcanic fields ($<10^4$ km²).

Figure 2: Volcanic rates grouped by petrotectonic setting for all locations in Tables 1 and 2. Shaded boxes represent the range of one standard deviation from the mean rate. The black bars show the minimum and maximum rates for each setting. For all settings, mean Q_e is skewed toward high values, which may imply a natural upper limit set by magma generation but no lower limit.

Figure 3: Repose interval between the end of one eruption and the start of the next, and range of SiO_2 content of lavas for locations in Table 4. Error bars represent the high and low values of the data. The points represent the mean repose interval and the middle of SiO_2 range. Solid line represents the best fit to a least-squares regression for an exponential equation which yields $t_{\text{repose}} = 10^{-6} * \exp(X/2.78)$. The e-folding factor of 2.78 indicates that repose time increases by a factor of ~ 3 for each ~ 3 wt % increase in silica.

Figure 4: Cartoon of a simplified volcanic system representing storage, and the processes affecting the volume of magma available for eruption. At some depth below the volcano, a volume of magma is stored in a liquid/crystal mush magma chamber. Inputs to the system are by recharge, a function of the magma upwelling rate, and assimilation of host rock. Outputs are by eruption or solidification of the magma by cooling within the magma chamber. A closed volcanic system in this context is one that receives no input.

Figure 5: Cartoon depicting a time-sequence of a simplified volcano that is closed to mass and advected heat between individual eruptions. The arrows indicate mass inputs and outputs. Eruptible magma is represented by the white oval, the lath pattern is cooling and crystallizing magma, and the stipple is country rock. Time t_0 shows the pre-existing conditions, while the sequence begins with the eruption at t_1 which removes the eruptible magma from the magma chamber. Recharge occurs at t_2 . Cooling during the storage period, shown in t_3 , is the interval between recharge and eruption (t_2 - t_4). There must be enough magma left at t_4 to equal the known volume of eruption. The repose period, as calculated for Figure 6, is the interval t_1 - t_4 . This model assumes that magma is fed into the system in isolated batches, as discussed in the text.

Figure 6: Openness of selected volcanic centers with well constrained eruptive volumes and repose intervals based on simple 1-D Stefan analysis. Each point, color coded by volcano, represents the repose interval between preceding an eruption and the solidification time for the erupted volume to completely crystallize before erupting. The volume of magma in storage is taken from the intrusive:extrusive ratio in Table 4 or assumed to be 5:1 if unavailable. The colored lines represent cutoff values for the amount of time magma may spend cooling and crystallizing in storage compared to the repose period. Points that plot below the line demand thermodynamically open systems that experience magma recharge prior to eruption. Points above the line may be closed in the sense that multiple eruptions could come from the same batch of magma without

additional input. Note that this does not require that these volcanoes act as closed systems.

Table 1: Rates and Volumes of Basaltic Volcanism

Location (Volcano Name)	Duration (Ma)	Extrusive Volume (km ³)	Volume Extrusion Rate Q _e (km ³ a ⁻¹)	Mass Extrusion Rate (kg a ⁻¹)	Bulk SiO ₂	Petrotectonic Setting	Notes	Reference
<i>Area < 10⁴ km² (Individual Volcanoes / Small Volcanic Fields)</i>								
Ascension	1.500	90	6.00E-05	1.49E+09	48	oceanic hotspot	Rough estimate of volumes from topography; rates constrained by a few K-Ar dates since 1.5 Ma.	[Gerlach, 1990; Nielson and Sibbett, 1996]
Auckland, New Zealand	0.140	2	1.07E-05	2.89E+07	B	Continental volcanic field	Volume calculated from thickness and areal extent based on field mapping and boreholes for 49 volcanic centers and adjusted to DRE volume. Active for last 140 ka based on K-Ar, thermo-luminescence, and ¹⁴ C dates.	[Allen and Smith, 1994]
Bouvet	0.700	28	4.00E-05	4.59E+08	48	oceanic hotspot	Very rough estimate of volume from island topography; active for past 0.7 Ma.	[Gerlach, 1990]
Camargo, Mexico	4.64	120	2.6E-05	7.02E+07	B	Continental volcanic field	Constraints from K-Ar dates from 4.73±0.04 Ma to 0.09±0.04 Ma. Volume based on an	[Aranda-Gomez et al., 2003]

La Palma, Canary Islands	0.123	125	1.0E-03	2.70E+09	48	oceanic hotspot	area of 3000 km ² and average thickness of 40 m Detailed field observations, mapping, and ³⁹ Ar/ ⁴⁰ Ar dating of uneroded Cumbre Viejo indicate activity since 123±3 ka.	[<i>Carracedo et al.</i> , 1999; <i>Guillou et al.</i> , 1998]
Santo Antao, Cape Verdes	1.750	68	4.00E-05	1.08E+08	48	oceanic hotspot	Rates from main shield-building stage Cha de Morte volcanics deposited between 2.93±0.03 and 1.18±0.01 Ma (³⁹ Ar/ ⁴⁰ Ar ages) and field mapping.	[<i>Plesner et al.</i> , 2002]
Coso, CA	1.500	24.3	1.60E-05	5.40E+12	57	continental volcanic field	Field mapping estimate of 23-25.5 km ³ erupted between 4.02±0.06 and 2.52±0.05 Ma (K-Ar ages).	[<i>Duffield et al.</i> , 1980]
Crater Flat, Nevada	3.700	10	3.7E-05	9.99E+07	B	continental volcanic field	Comprehensive study of volcanism in southern Nevada. Volumes from topography and field mapping, ages constrained to last 3.7 Ma mainly by ⁴⁰ Ar/ ³⁹ Ar.	[<i>Perry et al.</i> , 1998]
Edgecumbe	0.607	32	5E-05	1.35E+08	53	continental arc	Oldest age is K-Ar 611±74 ka; youngest is radiocarbon date	[<i>Crisp</i> , 1984; <i>Riehle et al.</i> ,

Eifel Volcanic field	0.690	2	2.14E-06	5.79E+06	B	continental volcanic field	4030±90 a. Volume based on detailed geologic mapping and accounting for DRE volumes for lavas and pyroclastic deposits. Volumes from field mapping. Activity 0.7 to 0.01 Ma based on ⁴⁰ Ar/ ³⁹ Ar and tephrochronology.	1992] [Mertes and Schmincke, 1985]
Erebus	0.250	4.00E-03	4.0E-03	1.08E+10	B	Continental arc	Volumes based on topography and assumed erosion, age constraints from ³⁹ Ar/ ⁴⁰ Ar dates.	[Esser et al., 2004]
Erebus	0.950	1.20E-03	1.2E-03	3.24E+09	B	Continental arc	Rough estimate of volume for proto-Erebus from topography and age constraints from ⁴⁰ Ar/ ³⁹ Ar dates.	[Esser et al., 2004]
Fernando de Noronha	12.000	60	5.00E-06	1.35E+07	48	oceanic hotspot	Approximate duration of volcanism 14 to 2 Ma.	[Gerlach, 1990]
Gough	2.42	99	4.09E-05	1.10E+08	48	oceanic hotspot	K-Ar ages from 2.55±0.51 to 0.13±0.02 Ma. Volume of basaltic shield does not include estimate of eroded volume prior to trachyte phase.	[Chevallier, 1987; Maund et al., 1988]
Juan Fernandez	1.000	72	7.20E-05	1.94E+08	48	oceanic	Approximate duration of volcanism 3 to 4 Ma.	[Gerlach,

						hotspot	Ages constrained by K-Ar dates.	[1990]
Kilauea	0.4	20000	5.00E-02	1.35E+11	48	oceanic hotspot	Volume estimate from drillhole stratigraphy and topography for past 0.4 Ma, based on K-Ar ages.	[<i>Quane et al., 2000</i>], [<i>Dvorak and Dzurisin, 1993</i>]
Kluychevskoy	0.010	275	2.70E-02	7.29E+10	B	continental arc	Volume based on cone is 275±25 km ³ and does not include ejecta beyond cone.	[<i>Crisp, 1984</i>]
Kohala, Hawaii	0.400	14000	3.50E-02	9.45E+10	B	oceanic hotspot	Volume estimate from bathymetry and topographic maps for past 0.4 Ma, based on K-Ar ages.	[<i>Crisp, 1984</i>]
Koolau, Oahu	0.600	20900	3.50E-02	9.45E+10	B	oceanic hotspot	Volume estimate from bathymetry and topographic maps for past 0.6 Ma, based on K-Ar ages.	[<i>Crisp, 1984</i>]
La Gomera, Canary Islands	1.4	350	2.5E-04	6.75E+08	B	oceanic hotspot	Rates obtained for main shield building stage. Volume calculated from DEM and field mapping for period of 9.4-8.0 Ma (K-Ar dates and paleomagnetic stratigraphy).	[<i>Paris et al., 2005</i>]
Lunar Crater, NV	5.700	100	1.70E-05	4.59E+07		Continental Volcanic field	Approximately 100 km ³ erupted over the past 5.7 Ma.	[<i>Crisp, 1984</i>]

Mauna Kea, Hawaii	0.300	24800	8.30E-02	2.24E+11	46	oceanic hotspot	Volume estimate from bathymetry and topographic maps for past 0.3 Ma, based on K-Ar ages.	[Crisp, 1984]
Mauna Loa, Hawaii	0.004	80	2.00E-02	5.40E+10	48	oceanic hotspot	Volume estimate from bathymetry and topographic maps for past 4 ka, based on K-Ar ages.	[Lipman, 1995]
Mauna Loa, Hawaii	0.500	42500	8.50E-02	2.30E+11	51	oceanic hotspot	Volume estimate from bathymetry and topographic maps for past 0.5 Ma, based on K-Ar ages.	[Crisp, 1984]
Mt. Cameroon	3.0	1500	5.00E-04	1.35E+09	45	continental hotspot	Rough estimate of volume for entire volcano, age constraints approximate activity from <3 Ma to present.	[Fitton and James, 1986; Marzoli et al., 2000]
Ocate, New Mexico	4.0	86	2.1E-05	5.67E+07	B	Continental Rift	Lavas erupted from 4.8 to 0.8 Ma, based on whole rock K-Ar dates. Approximate volume from field mapping. Older deposits (5.5 to 8.1 Ma) are substantially eroded so these are excluded here.	[Nielsen and Dungan, 1985]
Reunion	2.000	4800	2.40E-03	5.67E+11	48	oceanic hotspot	Based on a volcanic rate of $2.4 \pm 0.4 \text{ km}^3/\text{ka}$ and geochronology from early K-Ar dates for bulding the island	[Gerlach, 1990]

Ross	4.000	4800	1.20E-03	6.48E+09	48	oceanic hotspot	over the past 2 Ma. Based on a volcanic rate of $1.2 \pm 0.2 \text{ km}^3/\text{ka}$ for bulding the island over an estimated period of 0-4 Ma.	[<i>Gerlach, 1990</i>]
San Francisco Volcanic Field, AZ	5.000	525	1.05E-04	2.84E+08	B	Continental Volcanic field	Volume of small basaltic cinder cones and flows and larger silicic cones estimated from field mapping over past 5 Ma based on K-Ar dates.	[<i>Tanaka et al., 1986</i>]
Sao Miguel, Azores	0.00455	4.5	9.90E-04	2.67E+09	B	oceanic hotspot	Volume of 4.5 km^3 , DRE, from field mapping erupted over past 4.55 ka based on ^{14}C ages.	[<i>Crisp, 1984</i>]
Servilleta Basalt	1.0	200	2.0E-04	5.40E+08	B	Continental rift	Estimate of volume based on extent (200 km^2) and average thickness of flows (50 m) which range from 10 to 175 m thick. Eruptions in middle-to-late Pliocene is $1.0 \pm 0.5 \text{ Ma}$ based on K-Ar dates.	{ <i>Dungan, 1986 #386</i> }
Skye, British Tertiary Igenous Province	1.600	2300	1.44E-03	3.88E+09	B	Continental rift	Estimate of volume based on areal extent (1550 km^2) times average thickness (1.5 km) of deposits. Volcanic activity	[<i>Fowler et al., 2004</i>]

Springerville, Arizona	1.8	300	1.67E-04	4.51E+08	48	Continental Volcanic field	between 60.53±0.08 Ma and 58.91±0.06 Ma based on U-Pb zircon ages. Volumes from geologic mapping and borehole data. Eruptive period 0.3-2.1 Ma from K-Ar and magnetic polarity ages.	[Condit et al., 1989]
St. Helena	8.000	192	2.40E-05	7.29E+09	48	oceanic hotspot	Based on a volcanic rate of 0.24±0.12 km ³ /Ma for bulding the island over an estimated period of 7- 15 Ma.	[Gerlach, 1990]
Tatara, Chile	0.071	22	3.1E-04	8.37E+08	BA	continental arc	Estimates from field mapping, K-Ar and ⁴⁰ Ar/ ³⁹ Ar ages. Eruption time interval from 90 to 19 ka; units older than 90 ka are highly eroded	[Singer et al., 1997]
Tolbachik <i>Area > 10⁴ km² (large volcanic fields / arcs)</i>	0.010	69	6.90E-03	6.48E+08	B	continental arc	From rough estimate of average eruption rates over 2-10 ka and 2 ka to present.	[Crisp, 1984]
Baikal (Vitim)	10	5000	5.0E-04	1.35E+09	B	continental rift	Rough estimate of volumes and rates constrained by very limited K-Ar dates. Eruptive period 16.6-	[Johnson et al., 2005]; [Crisp, 1984]

Canary Islands	20.000	150000	7.50E-03	1.08E+08	B	oceanic hotspot	6.6 Ma. Age of oldest shield-building activity is uncertain. Oldest dated subaerial lava is 20 Ma (K-Ar) but oldest submarine activity could be 3X older.	[Crisp, 1984; Hoernle and Schmincke, 1993]
Caribbean Plateau	3.000	4000000	1.33E+00	1.08E+08	50	ocean plateau	Volume constraints from bathymetry and a drillhole. Eruptions from 91 to 88 Ma based on $^{40}\text{Ar}/^{39}\text{Ar}$ ages.	[Courtillot and Renne, 2003; Sinton et al., 1998]
Central Atlantic Basalt Province	4.000	2000000	5.00E-01	5.94E+09	50	continental flood basalt	Rough estimate of volume based on extent including Eastern North America, western Africa and Europe. Eruption between 197-201 Ma from a variety of sources ($^{40}\text{Ar}/^{39}\text{Ar}$, U-Pb, biostratigraphy)	[Courtillot and Renne, 2003]
Central Oregon p/100 km	1.0	163	1.63E-04	4.40E+08	B	continental arc	330 km ³ from mafic volcanoes and 180 km ³ from composite volcanoes for past 1 Ma. Uncertainties 10%-30% of volume. Adjusted for 300 km length of arc.	[Sherrod et al., 1990]
Central Oregon	2.0	750	3.75E-04	1.01E+09	53	continental arc	Volume estimated from field mapping and probable eroded volume at 2150 km ³	[Crisp, 1984]

Columbia River Basalt (Grande Ronde Basalt)	1.4	148600	1.06E-01	2.86E+11	B	continental flood basalt	and adjusted for 300 km arc. K-Ar age dates cluster in the period from 4 to 6 Ma. Volume estimate from field mapping and borehole thickness data. Lavas were erupted 17-15.6 Ma based on $^{40}\text{Ar}/^{39}\text{Ar}$ and K-Ar ages.	[Reidel et al., 1989]
Columbia River Basalt	11.5	174300	1.54E-02	4.32E+06	50	continental flood basalt	Volume estimate from field mapping and borehole thickness data for $174,300 \pm 27,900 \text{ km}^3$. Lavas were erupted 17.5-6 Ma based on $^{40}\text{Ar}/^{39}\text{Ar}$ and K-Ar ages.	[Tolan et al., 1989]
Deccan Traps	1.000	2000000	2.00E+00	8.91E+08	50	continental flood basalt	Eruptive period 65-66 Ma. There is a fair amount of controversy over the duration of activity.	[Courtillot and Renne, 2003]
E. Australia	60.000	20000	3.30E-04	2.59E+10	B	continental flood basal	Volume estimate from geologic mapping. Extrusion rate approximately constant for past 60 Ma. Only slight erosion for deposits less than 37 Ma.	[Crisp, 1984]
East Pacific Rise (p/100 km)	1.000	9600	9.60E-03	1.89E+10	50	ocean spreading	Volume calculated by multiplying area from	[Karson, 1998],

							spreading rate and given length, by extrusive layer thickness obtained from reflection seismic and stratigraphic mapping. Seismic Layer 2A assumed equal to extrusive layer thickness.	[Harding <i>et al.</i> , 1989], [Becker <i>et al.</i> , 1989]
Eastern Snake River Plain	3.000	21000	7.00E-03	7.02E+09	B	continental hotspot	Rough estimate for past 3 Ma, with no estimate of uncertainties.	[Crisp, 1984]
Eithiopia-Yemen Traps	1.500	1200000	8.00E-01	2.70E+12	50	continental flood basalt	Eithopian traps are 0.7 Mkm ³ and Yemen traps are 1.2 Mkm ³ . Erupted from 29.5 to 31 Ma based on ⁴⁰ Ar/ ³⁹ Ar and magneto-stratigraphy.	[Courtillot and Renne, 2003]
Emeishan	1.000	1000000	1.00E+00	2.21E+10	50	continental flood basalt	Rough estimate of volume from reconstruction of original area (5 Mkm ²) and thickness (2 km). Ages from ⁴⁰ Ar/ ³⁹ Ar and U-Pb are somewhat uncertain. Stratigraphic age is 258 Ma.	[Courtillot and Renne, 2003]

Faeroe Islands	3.5	4200	1.20E-03	3.24E+09	49	oceanic hotspot	Volume is rough estimate based on area of the islands, with 3 km thickness of lava pile. Unknown amount of original volume removed by glaciers, so volume is an underestimate. Ages based on $^{40}\text{Ar}/^{39}\text{Ar}$ and paleomagnetic dating.	[Crisp, 1984; Riisager et al., 2002]
		31					Uniform rate of $1.5\text{E}-03 \text{ km}^3/\text{a}$ from 15 to 7 ka, then an increase to $2.8\text{E}-03 \text{ km}^3/\text{a}$ from 7 to 2 ka. Lava flow area mapped and multiplied by average flow thickness to derive volumes for each of 38 individual flows. Age constraints from radiocarbon and paleomagnetic dating.	
Great Rift, Snake River Plain, Idaho	0.013		2.40E-03	6.48E+09	54	continental hotspot	Comprehensive assessment of volcano volumes using bathymetry. K-Ar ages.	[Kuntz et al., 1986]
Hawaii-Emperor Seamounts	73.600	1080000	1.50E-02	4.05E+10	48	oceanic hotspot	Volumes of postglacial eruptions over the past 10-12 ka, constrained by radiocarbon and tephrochronology.	[Crisp, 1984]
Iceland	0.011	484	4.4E-02	1.19E+11	50	oceanic hotspot		[Crisp, 1984]

Iceland	1.000	20000	2.00E-02	5.40E+10	B	oceanic hotspot	Based on total volume of Iceland divided by age of volcanism.	[Crisp, 1984]
Ireland	5.500	2000	3.60E-04	9.72E+08	B	Continental rift	Eruptive period from 66 Ma to 60.5±0.5 Ma estimated from K-Ar and ⁴⁰ Ar/ ³⁹ Ar ages. Volume estimated from the total area of 4000 km ² and average thickness of 0.5 km.	[Crisp, 1984]
Juan de Fuca Ridge (p/ 100 km)	1.000	9000	9.00E-03	2.43E+10	50	ocean spreading	Based on stratigraphic mapping of the extrusive layer thickness where exposed by faults, and the average spreading rate.	[Karson, 1998]
Kamchatka	0.250	8700	3.50E-02	6.48E+10	B	continental arc	Estimate of erupted volume between 0.85-0.6 Ma corrected for DRE.	[Crisp, 1984]
Kamchatka (basalts)	0.850	20660	2.40E-02	9.45E+10	B	continental arc	20660±300 km ³ erupted over past 0.08 Ma (from mainly radiocarbon ages). Overall rate calculated from a detailed assessment of rates as a function of time and type of volcanism.	[Crisp, 1984]
Kamchatka (basalts)	0.080	6140	7.70E-02	2.08E+11	B	continental arc	Rate calculated for just the basaltic volume erupted over the past	[Crisp, 1984]

Karoo-Farrar	6.000	2500000	4.16E-01	1.12E+12	50	continental flood basalt	0.08 Ma The volume is highly uncertain due to erosion, and the duration from 184 Ma to 178 Ma is based on $^{40}\text{Ar}/^{39}\text{Ar}$ ages.	[<i>Courtillot and Renne, 2003; Jourdan et al., 2005</i>]
Kenya (basalts)	2.500	15580	6.20E-03	9.45E+09	B	continental rift	Volume from geologic mapping and pre-erosional estimates for past 2.5 Ma, based on K-Ar and $^{40}\text{Ar}/^{39}\text{Ar}$ ages.	[<i>Crisp, 1984</i>]
Kenya (basalts)	4.500	23000	5.10E-03	1.38E+10	B	continental rift	Volume from geologic mapping and pre-erosional estimates for 7-2.5 Ma, based on K-Ar and $^{40}\text{Ar}/^{39}\text{Ar}$ ages. Uncertainties larger for older deposits.	[<i>Crisp, 1984</i>]
Kenya (basalts)	11.000	39000	3.50E-03	1.67E+10	B	continental rift	Volume from geologic mapping and pre-erosional estimates for 23-12 Ma, based on K-Ar and $^{40}\text{Ar}/^{39}\text{Ar}$ ages. Uncertainties larger for older deposits.	[<i>Crisp, 1984</i>]
Kenya and Tanzania	2.500	40470	1.60E-02	4.32E+10	B	continental rift	Volume ($40,470 \pm 7680 \text{ km}^3$) from geologic mapping and pre-erosional estimates for past 2.5 Ma, based on K-Ar and $^{40}\text{Ar}/^{39}\text{Ar}$ ages.	[<i>Crisp, 1984</i>]

Kenya and Uganda	11.000	108375	9.80E-03	2.65E+10	B	continental rift	Volume (108,375±23,125 km ³) from geologic mapping and pre-erosional estimates for 23 to 12 Ma, based on K-Ar and ⁴⁰ Ar/ ³⁹ Ar ages.	[Crisp, 1984]
Kerguelen Archipelago	11.000	99000	9.00E-03	5.94E+08	50	oceanic hotspot	Rough estimate of volume for island based on topography and bathymetry for 29.26±0.87 to 24.53±0.29 Ma, based on ⁴⁰ Ar/ ³⁹ Ar ages.	[Nicolaysen et al., 2000]
Kerguelen Island	26.000	5720	2.20E-04	2.43E+10	48	oceanic hotspot	Based on a volcanic rate of 0.22±0.01 km ³ /ka for bulding the island over an estimated period from 27 Ma to 1 Ma.	[Gerlach, 1990]
Kerguelen-Rajmahal- Bunbury	10.000	6000000	6.00E-01	1.62E+12	50	continental flood basalt	Grouped based on geochemical similarity. Erupted at 119-109 Ma.	[Courtillot and Renne, 2003]
Madagascar	4.000	4400000	1.10E+00	2.97E+12	50	continental flood basalt	Rough estimate of volume from area and thickness; erupted from 86-90 Ma based on ⁴⁰ Ar/ ³⁹ Ar dating.	[Courtillot and Renne, 2003]
Mid-Atlantic (p/ 100 km)	1.000	1500	1.50E-03	4.05E+09	50	Ocean spreading	Volume calculated by multiplying area from	[Tolstoy et al., 1993]

							spreading rate and given length, by extrusive layer thickness obtained from reflection seismic. Seismic Layer 2A assumed equal to extrusive layer thickness.	[Tucholke et al., 1997], [Hoofst et al., 2000]
Midland Valley, Scotland	27.500	6400	2.3E-04	6.21E+08	B	continental rift	Highly uncertain estimate of volume (4800 to 8000 km ³) erupted over 25-30 Ma during Carboniferous Period. Volume and age range estimates from Crisp [Crisp, 1984] corrected here.	[Crisp, 1984]
Modoc Basalt	5.000	2550	5.10E-04	7.59E+08	B	continental arc	Volume estimate from 1950 to 3150 km ³ based on field mapping. K-Ar ages from 5 to 10 Ma.	[Crisp, 1984]
Ninetyeast Ridge	40.000	7200000	1.80E-01	1.08E+10	48	oceanic hotspot	Rough estimate of volume for whole ridge based on topography and bathymetry for 38 to 83 Ma, based on ⁴⁰ Ar/ ³⁹ Ar ages.	[Duncan, 1991; Nicolaysen et al., 2000]
Ninetyeast Ridge	40.000	24000000	6.00E-01	4.86E+11	48	oceanic hotspot	Estimate for whole ridge based area and thickness of volcanic extrusive layer interpreted	[Grevemeyer et al., 2001]

North Atlantic Tertiary Volcanics 1	3.000	2000000	6.67E-01	1.62E+12	50	continental flood basalt	from seismic profiles. Rough volume estimate for the period of 62-59 Ma based on an extensive suite of dates including $^{40}\text{Ar}/^{39}\text{Ar}$ and U-Pb ages.	[<i>Courtillot and Renne, 2003</i>]
North Atlantic Tertiary Volcanics 2	3.000	2000000	6.67E-01	1.62E+12	50	continental flood basalt	Conservative estimate of extrusive volume for the period of 57-54 Ma based on $^{40}\text{Ar}/^{39}\text{Ar}$ and U-Pb ages. Some estimates include ~9.9 Mkm ³ of total igneous material.	[<i>Courtillot and Renne, 2003</i>]
Ontong-Java Plateau	2.000	6000000	3.00E+00	1.80E+12	50	ocean plateau	Total, corrected volume of extruded lavas at 122±1 Ma. Total volume of plateau is 44.4 Mkm ³	[<i>Courtillot and Renne, 2003</i>], [<i>Neal et al., 1997</i>]
Parana-Etendeka	0.600	2300000	3.83E+00	2.16E+08	50	continental flood basalt	Volume calculated from surface area (1.5 Mkm ²) and average thickness of flows (36 km). Total duration of trap volcanism is constrained to 0.6±1 Ma at 133±1	[<i>Courtillot and Renne, 2003</i>], [<i>Renne and Basu, 1991</i>]

							Ma ago by $^{40}\text{Ar}/^{39}\text{Ar}$ dates.	
Parana 1	3.000	90000	3.00E-02	1.04E+13	50	continental flood basalt	First phase of basaltic volcanism. Rough volume estimate from average flow thickness and extent. Ages constrained by numerous $^{40}\text{Ar}/^{39}\text{Ar}$ dates	[<i>Stewart et al.</i> , 1996]
Parana 2	2.000	260000	1.30E-01	2.16E+11	50	continental flood basalt	Second phase of basaltic volcanism. Rough volume estimate from average flow thickness and extent. Ages constrained by numerous $^{40}\text{Ar}/^{39}\text{Ar}$ dates	[<i>Stewart et al.</i> , 1996]
Parana 3	2.000	420000	2.10E-01	8.10E+10	50	continental flood basalt	Third phase of basaltic volcanism. Rough volume estimate from average flow thickness and extent. Ages constrained by	[<i>Stewart et al.</i> , 1996]

Parana 4	3.000	30000	1.00E-02	3.51E+11	50	continental flood basalt	numerous $^{40}\text{Ar}/^{39}\text{Ar}$ dates Fourth phase of basaltic volcanism. Rough volume estimate from average flow thickness and extent. Ages constrained by numerous $^{40}\text{Ar}/^{39}\text{Ar}$ dates	[<i>Stewart et al.</i> , 1996]
Rio Grande Rise	37.000	11100000	3.00E-01	2.70E+10	48	oceanic hotspot	Volume estimated from bathymetry and subsidence.	[<i>Gallagher and Hawkesworth</i> , 1994]
San Juan Mountains (basalts)	19.800	1020	5.10E-05	3.24E+09	B	Continental Volcanic field	Volume estimated from field mapping, includes estimate of eroded volume. K- Ar ages range from 23.4 to 3.6 Ma.	[<i>Crisp</i> , 1984]
Siberia	32.000	750000	2.70E-03	1.73E+10	B	continental flood basalt	Volume highly uncertain: 575,000 to 1,150,000 km ³ erupted from 248 to 216 Ma.	[<i>Crisp</i> , 1984]
Siberian Traps	1.000	3000000	3.00E+00	2.43E+09	50	continental	Volume from reconstruction of	[<i>Courtillot and Renne</i> ,

						flood basalt	original total area of 4 Mkm ² and preserved average flow thickness. Erupted during 1 Ma at about 250 Ma based on magnetic stratigraphy, U-Pb, and ⁴⁰ Ar/ ³⁹ Ar ages.	2003], [<i>Renne and Basu</i> , 1991]
Tasmania	44.500	400	9.40E-06	8.10E+12	B	continental rift	Duration from 47.5±7.5 to 2.55±2.45 Ma.	[<i>Crisp</i> , 1984]
Tibesti Massif	64.000	2680	4.20E-05	2.54E+07	55	continental hotspot	Rough estimate of total volume from 65 to 0.95±0.85 Ma. Volume estimated from detailed field mapping of uneroded young volcanics broken out by lava type and corrected to DRE. A total of 25 km ³ of basalts were erupted in shields, cones, and tephra along 50 km of arc length. Extensive suite of dates from ⁴⁰ Ar/ ³⁹ Ar, K-Ar, and radiocarbon. Rates only for volcanics of past 1.0 Ma.	[<i>Crisp</i> , 1984]
Zitacuaro-Valle de Bravo	1.000	24	2.40E-05	1.13E+08	50	continental arc		[<i>Blatter et al.</i> , 2001]

Table 2. Rates and Volumes of Silicic Volcanism

Location	Duration (Ma)	Extrusive Volume (km ³)	Volume Extrusion Rate Q _e (km ³ a ⁻¹)	Mass Extrusion Rate (kg a ⁻¹)	SiO ₂ Wt%	Petrotectonic Setting	Notes	Refs
<i>Area < 10⁴ km² (Individual Volcanoes / Small Volcanic Fields)</i>								
Alban Hills, Italy	0.561	290	5.2E-04	1.33E+09	A	Continental arc	Geologic map. Some ages from thermoluminescence. Period of eruptions 580 ka to 19 ka. Not corrected for DRE. Unknown amount of erosion.	[Chiarabba et al., 1997]
Asama	0.030	37	1.20E-03	8.61E+08	A	oceanic arc	37±7 km ³ erupted over past 0.03 Ma	[Crisp, 1984]
Avachinsky, USSR	0.060	100	1.70E-05	1.62E+08	BA	continental arc	Rough estimate excluding ejecta beyond cone.	[Crisp, 1984]
Ceboruco-San Pedro	0.8	80.5	8.05E-5	2.05E+08	A	continental arc	Volume determinations 80.5±3.5 km ³ from field mapping, digital topography, and orthophotos. Only minor erosion.	{Frey, 2004 #387}

Ceboruco-San Pedro	0.1	60.4	6.04E-4	1.54E+09	A	continental arc	Age from numerous $^{40}\text{Ar}/^{39}\text{Ar}$ dates. Volume determinations from field mapping, digital topography, and orthophotos. Only minor erosion. Age from numerous $^{40}\text{Ar}/^{39}\text{Ar}$ dates.	{Frey, 2004 #387}
Clear Lake, California	2.050	73	3.50E-05	2.81E+09	64	Continental Volcanic Field	For period from 2.06-0.01 Ma. Volume includes estimate of eroded material.	[Crisp, 1984]
Coso, California	0.4	2.4	5.7E-06	1.34E+07	R	Continental Volcanic Field	Geologic mapping estimate of 0.9 km ³ of basalt and 1.5 km ³ of rhyolite erupted over past 0.4 Ma based on K-Ar ages.	[Bacon, 1982]
Davis Mountains, Texas	1.5	1525	1.0E-03	2.35E+09	R	Continental Volcanic Field	Detailed field mapping and $^{40}\text{Ar}/^{39}\text{Ar}$ ages from 36.8 to 35.3 Ma. No DRE correction applied, as deposits have low porosity.	[Henry et al., 1994]

								The actual total volume may be as high as 2135 km ³ , if buried lava flows over full extent of area suggested.	
								Volume estimated from detailed field mapping for eruptions over past 11 ka (tephrachronology)	[Togashi et al., 1991]
Fuji	0.011	88	8.00E-03	4.59E+08	BA	oceanic arc		Duration is an estimate for the age range 14.1-13.4 Ma, based on K-Ar and ⁴⁰ Ar/ ³⁹ Ar for the Mogan Formation.	[Crisp, 1984; Freundt and Schminke, 1995; Hoernle and Schminke, 1993]
Gran Canaria, Canary Islands	0.600	200	3.30E-04	7.76E+08	69	oceanic hotspot		Volume 150±50 km ³ erupted over past 0.4 Ma	[Crisp, 1984]
Hakone	0.400	150	3.70E-04	4.34E+09	A	oceanic arc		Volume 3.7±1.2 km ³ , eruptions from 4-1 ka.	[Crisp, 1984]
Kaimondake	0.003	4	1.30E-03	2.04E+10	A	oceanic arc		Rough estimate of volumes for rhyolite domes and flows based on field	[Moyer and Esperanca, 1989]
Kaiser Spring, Arizona	3.2	7.5	2.34E-06	5.50E+06	R	Continental Volcanic Field			

Kuju	0.015	9	6.00E-04	1.53E+09	A	oceanic arc	<p>mapping. No estimate for basalt flows. Eruptive activity from 8.8 to 12 Ma based on K-Ar dates.</p> <p>Volumes from field mapping and average thickness of flows, and isopach maps of tephras corrected for DRE. Age constraints from ^{14}C and tephrochronology. Rates estimated at 0.4-0.7 km³/ka. [Kamata and Kobayashi, 1997]</p> <p>DRE-corrected volume from geological mapping. Activity since 0.76 Ma based on $^{40}\text{Ar}/^{39}\text{Ar}$ dates. [Hildreth, 2004; McConnell et al., 1995]</p> <p>Age constraints from ^{14}C and K-Ar dates. Volume estimates from field mapping and</p>
Long Valley, CA	0.76	700	9.21E-04	2.16E+9	R	Continental Volcanic Field	
Mazama (Crater Lake), Oregon	0.340	101	2.97E-04	6.98E+08	R	Continental arc	

Misti	0.112	76.5	6.8E-04	1.73E+09	A	Continental arc	<p>estimates for erosion are 40-52 km³ for pre-caldera Mt. Mazama and 51-59 km³ erupted during caldera formation. A detailed chronology of eruptive events.</p> <p>Extensive geologic field mapping and ages from ⁴⁰Ar/³⁹Ar, plagioclase thermoluminescence, and ¹⁴C chronology. Volume of stratocones estimated at 70-83 km³. Not enough information to calculate DRE volume.</p> <p>[<i>Thouret et al.</i>, 2001]</p> <p>Very detailed assessment of rates as a function of time and type of eruption. Extensive set of whole rock K-Ar ages. Comprehensive geologic mapping with estimates of areas and potential range of pre-erosional thickness for 124 map units. Earliest ages are 940 ka, but most volume was erupted since 520 ka.</p>
Mt. Adams	0.520	303	5.8E-04	1.48E+09	A	continental arc	<p>[<i>Hildreth and Lanphere</i>, 1994]</p>

Mt Baker	1.290	161	1.25E-04	7.14E+09	60	continental arc	Very detailed assessment of rates as a function of time from 80 K-Ar and $^{40}\text{Ar}/^{39}\text{Ar}$ dates for past 1.29 Ma. Estimate for pre-erosional volume is $161 \pm 56 \text{ km}^3$ from detailed field mapping.	[Hildreth et al., 2003a]
Mt Griggs	0.292	35	1.21E-04	5.87E+11	54	oceanic arc	Total erupted volume estimated from detailed field mapping as $35 \pm 5 \text{ km}^3$ since $292 \pm 11 \text{ ka}$.	[Hildreth et al., 2003b]
Mt Katmai	0.890	70	7.0E-04	6.38E+10	61	oceanic arc	Total erupted volume estimated at $70 \pm 18 \text{ km}^3$ since $89 \pm 13 \text{ ka}$, although most volume has erupted since 47 ka .	[Hildreth et al., 2003b]
Mt Mageik	0.093	30	3.3E-04	7.05E+09	62	oceanic arc	Total erupted volume estimated from detailed mapping and pre-erosional estimates for the past 93 ka.	[Hildreth et al., 2003b]
Mt. St. Helens	0.040	79	1.98E-03	5.04E+09	A	Continental arc	Volumes include estimates of main cone, flank flows, pyroclastic flows, and rough estimate of pre-1980 tephra volumes corrected for DRE.	[Sherrod et al., 1990]
Oshima	0.025	33	1.50E-03	1.82E+08	A	oceanic arc	Total volume from cone $33 \pm 11 \text{ km}^3$ over the	[Crisp, 1984]

Ruapehu, New Zealand	0.25	300	1.20E-03	3.06E+09	A	Continental arc	past 25±15 ka. Volume estimate includes cone (146 km ³) plus reworked deposits on ring-plain. Age constraints from ⁴⁰ Ar/ ³⁹ Ar for eruptions since 250 ka.	[Gamble et al., 2003]
Sakurajima	0.014	25	1.80E-03	2.55E+12	A	oceanic arc	Total volume from cone 25±5 km ³ over the past 14±1 ka.	[Crisp, 1984]
Santorini	0.067	45	6.72E-04	1.58E+09	R	Oceanic arc	Rough estimates of volumes from detailed field mapping and reconstruction Minoan eruption and Skaros shield. Detailed chronology from radiocarbon, K-Ar, and ⁴⁰ Ar/ ³⁹ Ar dates indicates activity since 360 ka, and building Skaros shield began at 67±9 ka.	[Druitt et al., 1999]

Shiveluch	0.200	1000	5.00E-03	1.12E+09	A	continental arc	Rough estimate, does not include ejecta beyond cone.	[Crisp, 1984]
Sierra la Primavera	0.068	34	5.00E+04	1.48E+08	R	continental arc	Magma volume based on field mapping of 320 km ² study area, erupted over the period 0.095±0.005 Ma to 0.0275±0.0025 Ma from K-Ar ages.	[Crisp, 1984]
Soufriere Hills – South Soufriere	0.174	26	1.5E-04	3.83E+08	A	continental arc	Rate given includes DRE correction and assumed submarine deposits. Only minor erosion. Age from numerous ⁴⁰ Ar/ ³⁹ Ar dates indicate eruptions since 174±3 ka.	[Harford et al., 2002]
Taupo	0.027	73	2.76E-03	6.35E+09	74	continental arc	Eruptive volume calculated from detailed stratigraphic record and tephra isopach maps since the volcano's 26.5 ka caldera-forming eruption. Rates constrained by ¹⁴ C dates.	[Sutton et al., 2000]

Taupo	0.610	7044	1.10E-02	4.59E+09	R	continental arc	Includes area of pyroclastic sheets (20,000 km ²) from Taupo vents. Careful assessment of volumes from geologic mapping, erupted over the period 1.13 to 0.51 Ma. Ages are K-Ar, ¹⁴ C, and fission track.	[Crisp, 1984]
Taupo (recent)	0.050	350	7.00E-03	1.18E+10	R	continental arc	Includes Taupo and Okatina volcanic centers. Volume determined from geologic maps and tephra isopach maps, corrected for DRE, over past 50 ka (¹⁴ C ages).	[Crisp, 1984]
Terceira, Azores	0.023	5.46	2.40E-04	6.48E+07	60	oceanic hotspot	Minimum volume estimated from geological maps and corrected for DRE. Eruptions over past 23 ka constrained by ¹⁴ C dates.	[Crisp, 1984]
Tequila, Mexico	1.0	128	1.28E-04	3.26E+08	A	Continental arc	K-Ar dating, detailed geologic mapping, and	[Lewis-Kenedi et al.,

Timber Mountain, Nevada	2.8	4000	1.43E-03	3.36E+09	R	Continental Volcanic Field	digital elevation models provide minimum- maximum estimates for 49 eruptive units. Overall volume uncertainty is $128 \pm 22 \text{ km}^3$. Volume from large tuff deposits corrected to DRE. Duration from 12.8 Ma to ~10 Ma from $^{40}\text{Ar}/^{39}\text{Ar}$ sanidine and K-Ar. Volume for other minor volcanism in area not reported.	[Farmer et al., 1991]; [Bindeman and Valley, 2003]
Tongariro	0.275	60	2.2E-04	5.61E+08	A	continental arc	Based on a rough estimate of volume of the volcanic cone and K-Ar ages.	[Hobden et al., 1999]; [Hobden et al., 1996]
Trident Volcano	0.142	22	1.54E-04	1.18E+17	62	oceanic arc	Total eruptive volume of 22 ± 3 km^3 since 142 ± 15 ka based on K-Ar dates.	[Hildreth et al., 2003b]
Tungurahua	0.002	3	1.50E-03	9.18E+10	55-65	continental arc	Volumes from most recent edifice in	[Hall et al., 1999]

Twin Peaks, UT	0.39	12	3.1E-05	7.29E+07	76	Continental Volcanic Field	<p>volcanic complex based on estimates from field mapping and topography, erupting since 2215±90 years ago based on detailed tephrochronology and ¹⁴C dates. Volumes include distal tephras and are adjusted to DRE</p> <p>Minimum volume of 12 km³ of silicic magma erupted from 2.74±0.10 Ma to 2.35±0.08 Ma, based on K-Ar ages. [Crecraft <i>et al.</i>, 1981; Evans <i>et al.</i>, 1980]</p>
Valles	1.33	265	2.00E-04	2.59E+10	R	continental hotspot	<p>Volume constraints from mapping. Age constraints from K-Ar dates from 1.43±0.09 to 0.1 Ma [Crisp, 1984]</p>
Volcan San Juan	0.034	60	1.78E-03	1.65E+10	R	continental arc	<p>Combined volumes of main cone and adjacent satellite cone, from topographic since [Luhr, 2000]</p>

Yatsugatake	0.171	513	3.00E-03	3.92E+08	A	oceanic arc	33.75±1.8 ka. Volume estimates include very detailed isopach maps of tephra and DRE corrections. Estimate of volumes from tephra and rough estimate of volcano volumes. Age constraints from tephrochronology for Younger Yatsugatake, past 171 ka.	[Oishi and Suzuki, 2004]
<i>Area > 10⁴ km² (large volcanic fields / arcs)</i>								
Aleutians p/100 km extrusive only	3.500	350	1.00E-04	5.61E+09	A	oceanic arc	Detailed study of volumes in past 3-4 Ma indicate a total of 4700-10000 km ³ over an arc length of 2100 km	[Crisp, 1984]
Aleutians p/100km int+ext	80.000	272000	3.50E-03	8.93E+09	A	oceanic arc	Estimated from 80 Ma age of arc and approximate 34 km ³ /Ma/km volume excess of the arc over oceanic crust	[Crisp, 1984]

Altiplano-Puna Volcanic Complex	10	6120	6.12E-04	1.56E+09	A	Continental arc	No uncertainties given. Duration for the past 10 Ma.	[Francis and Hawkesworth, 1994]
Cascade Range p/100 km	2.0	1900	9.5E-04	2.42E+09	A	continental arc	Estimated for 0-2 Ma Quaternary volcanics in Northern California to southern British Columbia and 8 to 11 km ³ /km/Ma extrusion rate.	[Sherrod <i>et</i> <i>al.</i> , 1990]
Central Andes Volcanic Zone p/100 km	10.000	3740	3.74E-04	9.54E+08	60	continental arc	Volume estimated from volcano edifice volumes (1113 total) for past 10 Ma. No correction for erosion or distal tephras.	[Francis and Hawkesworth, 1994]
Central Andes Volcanic Zone p/100 km	1.000	159	1.59E-04	4.05E+08	60	continental arc	Volume from edifices active during past 1 Ma (246 total). Somewhat uncertain; ages based partly on geomorphological evidence.	[Francis and Hawkesworth, 1994]
Central Oregon p/100	4.000	12425	3.10E-03	3.09E+06	57	continental	Volume estimated	[Crisp, 1984]

km						arc	<p>from field mapping. K-Ar ages cluster in periods from 16 to 14 Ma and 11 to 9 Ma. Adjusted for length of arc of 200 km.</p> <p>Constrained as minimum volume from field mapping of Oligocene-Early Miocene deposits with K-Ar ages from 34 to 20 Ma. This estimate has more uncertainty than other entries for Central Oregon. Adjusted for length of arc of 200 km.</p>	
Central Oregon p/100 km	14.000	5000	3.60E-02	3.0E+07	62	continental arc	<p>Adjusted for length of arc of 200 km.</p> <p>Geologic mapping and detailed stratigraphy of 9 provinces to derive an volume estimated from areal coverage and thickness of representative units. Eruptive activity between 188±1 Ma and 142±4 Ma constraints from K-Ar</p>	[Crisp, 1984]
Chon Aike, South America	35.000	23000	6.57E-04	1.51E+09	R	Continental rift	<p>Eruptive activity between 188±1 Ma and 142±4 Ma constraints from K-Ar</p>	[Pankhurst et al., 1998]

East Nicaragua p/100 km	0.135	187	1.38E-03		60	continental arc	Total arc length is 130 km. Volume is an estimate of volcano volumes, and is not corrected for erosion or distal tephtras. Age constraints from tephrochronology.	[Patino et al., 2000]
El Salvador p/100 km	0.2	292	1.5E-03	3.52E+09	60	continental arc	Volume estimate of 736 km ³ for 252 km arc length for past 0.2 Ma. Volume is an estimate of volcano volumes, with no correction for erosion or distal tephtras.	[Patino et al., 2000]
Ethiopia	4.000	28125	7.00E-03	8.93E+07	R	continental rift	Volume of 28,125±5625 km ³ erupted from 5.5 to 1.5 Ma.	[Crisp, 1984]
Guatemala p/100 km	0.084	140	1.7E-03	4.34E+09	60	continental arc	Volume estimate of 163 km ³ for 116 km arc length. Volume is an estimate of volcano volumes, and is fairly uncertain with no correction for	[Patino et al., 2000]

Japan	0.250	2020	8.10E-03	1.02E+10	R	oceanic arc	erosion or distal tephtras. Age constraints from tephrochronology. Minimum volume estimate for the past 0.25 Ma [Crisp, 1984]
Japan	23.000	109400	4.76E-03	9.52E+09	R	oceanic arc	Volume estimated at $109,400 \pm 21,900$ km ³ based on cones of recent volcanoes, flow thickness maps, and average thickness of older volcanic deposits. Duration updated from Crisp [1984] to conform to Neogene timescale. [Crisp, 1984]
Kamchatka (silicic)	0.080	840	1.10E-02	1.02E+09	64	continental arc	840 ± 165 km ³ erupted over past 0.08 Ma. Detailed assessment of rates as a function of time and type of volcanism. [Crisp, 1984; Erlich and Volynets, 1979]
Kenya (phonolites)	2.500	28125	1.20E-02	4.95E+08	R	continental rift	Volume ($28,125 \pm 9375$ km ³) from geologic [Crisp, 1984]

Kenya (silicic)	2.500	4640	1.90E-03	9.44E+08	R	continental rift	mapping and pre-erosional estimates for past 2.5 Ma, based on K-Ar and $^{40}\text{Ar}/^{39}\text{Ar}$ ages. Volume (4640±930 km ³) from geologic mapping and pre-erosional estimates for 13.4 to 11 Ma, based on K-Ar and $^{40}\text{Ar}/^{39}\text{Ar}$ ages.	[Crisp, 1984]
Kenya (silicic)	4.500	20600	4.60E-03	9.64E+09	R	continental rift	Volume (20,600±4100 km ³) from geologic mapping and pre-erosional estimates for 7 to 2.5 Ma, based on K-Ar and $^{40}\text{Ar}/^{39}\text{Ar}$ ages.	[Crisp, 1984]
Kurile Islands	0.070	300	4.30E-03	1.90E+10	58	oceanic arc	Not corrected for porosity. No details on uncertainty.	[Crisp, 1984]
Kurile Islands p/100km int+ext	83.000	392500	4.75E-03	3.32E+09	58	oceanic arc	Very rough estimate for past 83 Ma.	[Crisp, 1984]
Lesser Antilles p/100	0.010	3	3.0E-04	7.65E+08	55	oceanic arc	Detailed volume estimates for	[Wadge,

km							individual islands with age constraints from tephrochronology. Volumes adjusted for 100 km of arc length	[1984]
Lesser Antilles p/100 km	0.100	40	4.0E-04	1.02E+09	55	oceanic arc	Detailed volume estimates for individual islands with age constraints from tephrochronology. Volumes adjusted for 100 km of arc length	[Wadge, 1984]
							Very rough estimate for an arc length of 620 km, where an estimated 39,500 km ³ DRE magma was erupted since 5 Ma. Volumes derived from topography, volcanic deposits, and volcanoclastic sediments.	
Marianas p/100km	5.000	6370	1.25E-03	1.10E+10	BA	oceanic arc		[Crisp, 1984]
Michoacan-	4.000	1090	2.73E-04	6.95E+08	53	continental	Volume of cinder cones and shields	[Hasenaka,

Guanajuato						arc	for past 4 Ma, based on K-Ar dates. calculated assuming symmetrical truncated cones and average flow thickness times mapped area of flow, all corrected to DRE based on vesicularity assumptions. Airfall ash volume was assumed 7.73 times the volume of the associated cone. No corrections made for erosion or burial.	[1994]
Michoacan-Guanajuato	0.04	30.5	7.6E-04	1.94E+09	53	continental arc	Same as above except volume of young cinder cones only. Volcanism since 40 ka based on constraints from K-Ar and ¹⁴ C.	[Hasenaka, 1994; Hasenaka and Carmichael, 1985]
Mongollon-Datil, New Mexico	17.0	40000	2.35E-03	5.53E+09	R	Continental volcanic field	Volume estimates based on area (20,000 km ²) times	[Davis and Hawkesworth, 1995]

North Costa Rica p/100 km	0.1	441	4.41E-03	3.19E+10	60	continental arc	average thickness of deposits (2-3 km). No correction for DRE or erosion. Period of activity estimated as 37-20 Ma, with some minor activity later. Over 50% of volume estimated as rhyolite, with a range of compositions for the remainder. Total arc length is 100 km. Volume estimated from volcano cone volumes, with no correction for erosion or distal tephras. Age constraints from radiometric dates.	[Patino et al., 2000]
North Queensland, Australia	105.000	6550	6.30E-05	1.12E+09	R	continental flood basalt	Period of eruptions was 345 to 240 Ma.	[Crisp, 1984]
San Juan Mountains	4.700	40000	8.51E-03	2.17E+10	60	Continental Volcanic field	Volume estimated from field mapping and includes estimate of eroded	[Lipman, 1984]

Sierra Madre Occidental p/100 km	15.000	48900	3.26E-03	3.8E+08	R	continental rift	<p>volume. K-Ar ages span 34.7 Ma to 30 Ma.</p> <p>Rough estimates of volumes, from reconstructed areal coverage and thickness from detailed stratigraphy, of main field (393 km³) and surrounding smaller fields over a total arc length of 1200 km. Ages constrained loosely to 38-23 Ma with some smaller eruptions as late as 16 Ma.</p>	[Aguirre-Diaz and Labarthe-Hernandez, 2003]
Twin Peaks-Cove Fort-Black Rock- Mineral Mtn	2.320	77	3.30E-05	6.50E+09	R	Continental Volcanic Field	<p>Volume 77±4 km³ erupted from 2.74±0.1 to 0.42±0.07 Ma based on K-Ar ages</p> <p>Volume is order-of-magnitude estimate based on outcrop and calculated volume of volcaniclastic sediment. Volcanic and intrusive activity occurred from 132 to 95 Ma, but the main phase of activity was 120 and 105 Ma.</p>	[Crisp, 1984]
Whitsunday, Australia	37	100000	2.7E-03	6.19E+09	R	continental rift		[Bryan et al., 1997]

Yellowstone	2.100	4980	2.37E-03	5.25E+09	74	continental hotspot	Detailed study of 71,000 km ² region from many years of fieldwork, geologic mapping, volcanic stratigraphy breaking out 3 large volcanic cycles. The estimated volume of all known rhyolites is estimated at 4730 km ³ and basalts 250 km ³ . No formal errors are given. Age constraints from an extensive suite of K-Ar and ⁴⁰ Ar/ ³⁹ Ar dates from 2.16±0.04 to 0.070±0.002 Ma.	[Christiansen, 2001]
Zitacuaro-Valle de Bravo p/100 km	1.000	115.6	1.16E-04	2.04E+09	60-65	continental arc	Volume estimated from detailed field mapping of uneroded young volcanics broken out by lava type and corrected to DRE. Total of 57.8 km ³ of andesite and dacite was erupted in cones, flows, and tephra. Arc length is 50 km. Extensive suite of dates from ⁴⁰ Ar/ ³⁹ Ar, K-Ar, and radiocarbon. Rates only for volcanics of past 1.0 Ma.	[Blatter et al., 2001]
Zitacuaro-Valle de Bravo p/100 km	1.000	11.4	1.14E-05	7.76E+07	BA	continental arc	Volume estimated from detailed field mapping of uneroded young	[Blatter et al., 2001]

volcanics broken out by lava type and corrected to DRE. Total of 5.7 km³ of basaltic andesite was erupted in cones, flows, and tephra. Arc length is 50 km. Extensive suite of dates from ⁴⁰Ar/³⁹Ar, K-Ar, and radiocarbon. Rates only for volcanics of past 1.0 Ma.

Table 3. Intrusive:Extrusive Ratios

Volcano	Intrusive	Extrusive	Ratio	Method	Reference
Aleutians	1073-1738 km ³ /km	627-985 km ³ /km	1:1-3:1*	Seismic and crystallization of Hidden Bay Pluton and related extrusives	[<i>Kay and Kay, 1985</i>]
Bushveld-Rooiberg, South Africa	1x10 ⁶ km ³	3x10 ⁵ km ³	3:1	Stratigraphic mapping. Cr and incompatible trace element analyses indicate that the total magma volume intruded was approximately 1x10 ⁶ km ³ .	[<i>Cawthorn and Walraven, 1998; Schweitzer et al., 1997; Twist and French, 1983</i>]
Central Andes, Peru	9-29x10 ⁴ km ³	2.25x10 ⁴ km ³	3:1-12:1	Extrusive from geologic mapping. Intrusive from mapping and gravity.	[<i>Francis and Hawkesworth, 1994; Haederle and Atherton, 2002</i>]
Challis Volcanic Field, Idaho	3.5x10 ³ km ³	4x10 ³ - 2.8x10 ⁴ km ³	>1:1-8:1	Very uncertain; Field and stratigraphic mapping; extrusive converted to DRE using 75% porosity; total plutonic thickness unk.	[<i>Criss et al., 1984</i>]

Coso Volcanic field, California	2.8 km ³ /Ma (basalt)	570 km ³ /Ma	1:200*	Extrusive from geologic mapping for past 0.4 Ma; intrusive rate based on current heat flow and estimates of local tectonic extension.	[Bacon, 1983]
	5.4 km ³ /Ma (rhyolite)		1:100*		
East Pacific Rise	7 km	0.5-0.8 km	5:1-8:1	Seismic; Stratigraphic Mapping	[Detrick <i>et al.</i> , 1993; Harding <i>et al.</i> , 1993; Karson, 2002]
Etna, Italy (1 Ma)	3x10 ² km ³	1x10 ² km ³	3:1	Seismic (estimate for ~0.1 Ma)	[Allard, 1997; Hirn <i>et al.</i> , 1991]
Etna, Italy (since 1975)	0.6 km ³	5.9 km ³	10:1	SO ₂ flux 1975-1995 AD	
Hawaiian-Emperor Seamount Chain	5.9x10 ⁶ km ³	1.1x10 ⁶ km ³	6:1*	Extrusive from topographic maps; intrusive from flexural models and seismic, averaged over the past 74 Ma	[Bargar and Jackson, 1974; Vidal and Bonneville, 2004]
Iceland	5 km	20-40 km	4:1-8:1	Seismic	[Bjarnason <i>et al.</i> , 1993; Darbyshire <i>et al.</i> , 1998; Menke <i>et al.</i> , 1998; Staples <i>et al.</i> , 1997]
Kerguelen Archipelago	9.9x10 ⁴ km ³	2.75x10 ⁶ km ³	28:1*	Seismic	[Nicolaysen <i>et al.</i> , 2000]
Kilauea, Hawaii	9x10 ⁻² km ³ /a	5x10 ⁻² km ³ /a	2:1	Drillhole Stratigraphy; Ground Deformation; Geologic Mapping	[Dvorak and Dzurisin, 1993; Quane <i>et al.</i> , 2000]
Long Valley, California	7.6x10 ³ km ³	7.5x10 ² km ³	10:1	Rough estimate from seismic tomography, stratigraphic mapping, drillholes, and gravity	[Hildreth, 2004; McConnell <i>et al.</i> , 1995; Weiland <i>et al.</i> , 1995]
Marquesas Islands	6.2x10 ⁵ km ³	3.3x10 ⁵ km ³	2:1*	Seismic	[Caress <i>et al.</i> , 1995]
Mauna Loa,	8x10 ¹ km ³	1.1-2.4x10 ²	>1:1-3:1	Stratigraphic mapping, for the 1877-	[Klein, 1982; Lipman, 1995]

Hawaii		km ³		1950 time period	
Mid-Atlantic Ridge	5.5-7 km	0.5-1.5 km	5:1-10:1	Seismic	[Hooft <i>et al.</i> , 2000]
Miyake, Japan	4 km ³	1.5x10 ⁻¹ km ³	3:1	Geodetic Modeling; SO ₂ emissions	[Kumagai <i>et al.</i> , 2001]
Mull Volcano, Scotland	1.3x10 ⁴ km ³	7.6x10 ³ km ³	2:1	Stratigraphic mapping	[Walker, 1993]
Ninetyeast Ridge	7-8 km	3-4 km	2:1	Seismic	[Grevemeyer <i>et al.</i> , 2001; Nicolaysen <i>et al.</i> , 2000]
Pinatubo, Philippines	60-125 km ³	3.7-5.3 km ³	11:1-34:1	Seismic, Stratigraphic Mapping	[Mori <i>et al.</i> , 1996; Wolfe and Hoblitt, 1996]
San Francisco Mountain, Arizona	94 km ³	500 km ³	6:1	Geologic mapping, estimated amount of eroded material included, and seismic low-velocity body with a volume of 300-700 km ³ .	[Tanaka <i>et al.</i> , 1986]
Twin Peaks, Utah	290-430 km ³	40-43 km ³	5:1-9:1	Geologic mapping, gravity and thermal modeling.	[Carrier and Chapman, 1981; Crecraft <i>et al.</i> , 1981; Evans <i>et al.</i> , 1980]
Yellowstone	6.5x10 ³ km ³	1.89x10 ⁴ km ³	3:1	Seismic; Stratigraphic Mapping	[Christiansen and Blank, 1972; Clawson <i>et al.</i> , 1989; Miller and Smith, 1999]

*values that include crustal underplating

Table 4: Repose Times at Selected Volcanic Centers

Volcano	Repose Time	Repose Min	Repose Max	Number of	wt % SiO ₂	wt % SiO ₂	Refs	Notes
---------	-------------	------------	------------	-----------	-----------------------	-----------------------	------	-------

	Avg (a)	(a)	(a)	Reposes in Record	min	max		
Colima	80	48	138	3	56	61	[<i>Luhr and Carmichael, 1980</i>]	four cycles of ac eruptions since 1
Etna	4	0.1	100	70	47	50	[<i>Tanguy, 1979; Wadge, 1977</i>]	Constrained by 1 to 2001 AD
Fogo, Cape Verde	20	1	94	27	40	42	[<i>Doucelance et al., 2003; Trusdell et al., 1995</i>]	Constrained by 1 to 1995 AD
Fuego	100	10	150	60	49	55	[<i>Martin and Rose, 1981</i>]	Constrained by 1 AD; eruptions o
Izu-Oshima	68	13	190	23	53	57	[<i>Koyama and Hayakawa, 1996</i>]	Detailed syn- an history from tep reposes since ca
Katla	46	13	80	20	46	50	[<i>Larsen, 2000</i>]	Last 11 centurie records
Kilauea	0.8	0.1	10	46	48	50	[<i>Klein, 1982</i>]	Constrained by 1 to 1979 AD
Mauna Loa	5	0.1	20	34	48	50	[<i>Klein, 1982</i>]	Constrained by 1 to 1984 AD
Mt Adams	150000	50000	320000	3	57	64	[<i>Hildreth and Fierstein, 1997; Hildreth and Lanphere, 1994</i>]	Major cone buil
Mt St Helens	8600	5000	15000	6	63	67	[<i>Doukas, 1990; Mullineaux, 1996</i>]	From 40 ka to p only
Ruapehu	30000	10000	60000	5	55	65	[<i>Gamble et al., 2003</i>]	Constrained by 4
Santorini	30000	17000	40000	12	58	71	[<i>Druitt et al., 1999</i>]	For major explo Both ⁴⁰ Ar/ ³⁹ Ar a

Taupo	2000	20	6000	28	72	76	[<i>Sutton et al.</i> , 2000]	radiocarbon age: Post-Oruanui er present
Toba	375000	340000	430000	3	68	77	[<i>Chesner and Rose</i> , 1991]	Reposes between since 0.8 Ma
Valles	335000	320000	350000	3	69	75	[<i>Doell et al.</i> , 1968; <i>Heiken et al.</i> , 1990]	Reposes based o pre-Bandelier tu and Valles calde
Yatsugatake	32000	10000	85000	5	53	63	[<i>Kaneoka et al.</i> , 1980; <i>Oishi and Suzuki</i> , 2004]	Plinian eruption; Tephrochronolog
Yellowstone	700000	600000	800000	3	75	79	[<i>Christiansen</i> , 2001]	Considers major

References

- Aguirre-Diaz, G.J., and G. Labarthe-Hernandez, Fissure Ignimbrites: Fissure-source origin for voluminous ignimbrites of the Sierra Madre Occidental and its relationship with Basin and Range faulting, *Geology*, 31 (9), 773-776, 2003.
- Allard, P., Endogenous magma degassing and storage at Mount Etna, *Geophysical Research Letters*, 24 (17), 2219-2222, 1997.
- Allen, S.R., and I.E.M. Smith, Eruption styles and volcanic hazard in the Auckland Volcanic Field, New Zealand, *Geosci. Repts. Shizuoka Univ.*, 20, 5-14, 1994.
- Aranda-Gomez, J.J., J.F. Luhr, T.B. Housh, C.B. Connor, T. Becker, and C.D. Henry, Synextensional Pliocene-Pleistocene eruptive activity in the Camargo volcanic field, Chihuahua, Mexico, *Geol. Soc. Am. Bull.*, 115, 298-313, 2003.
- Asimow, P.D., Steady-state mantle-melt interactions in one dimension; II, Thermal interactions and irreversible terms, *J. Petrol.*, 43 (9), 1707-1724, 2002.
- Bacon, C.R., Time-predictable bimodal volcanism in the Coso Range, California, *Geology*, 10, 65-69, 1982.
- Bacon, C.R., Eruptive history of Mount Mazama and Crater Lake Caldera, Cascade Range, U.S.A., *J. Volc. Geotherm. Res.*, 18, 57-115, 1983.
- Bacon, C.R., and M. Lanphere, The geologic setting of Crater Lake, Oregon, in *Crater Lake: An Ecosystem Study*, edited by E.T. Drake, G.L. Larson, J. Dymond, and R. Collier, pp. 19-27, Pacific Div. of the American Association for the Advancement of Science, San Francisco, 1990.
- Bargar, K.E., and E.D. Jackson, Calculated volumes of individual shield volcanoes along the Hawaiian-Emperor Chain, *Jour. Research U.S. Geol Survey*, 2, 545-550, 1974.
- Becker, K., H. Sakai, A.C. Adamson, J. Alexandrovich, J.C. Alt, R.N. Anderson, D. Bideau, R. Gable, P.M. Herzig, S. Houghton, H. Ishizuka, H. Kawahata, H. Kinoshita, M.G. Langseth, M.A. Lovell, J. Malpas, H. Masuda, R.B. Merrill, R.H. Morin, M.J. Mottl, J.E. Pariso, P. Pezard, J. Phillips, J. Sparks, and S. Uhlig, Drilling deep into young oceanic crust, Hole 504B, Costa Rica Rift, *Reviews of Geophysics*, 27, 79-102, 1989.
- Bindeman, I.N., and J.W. Valley, Rapid generation of both high and low d18O, large-volume silicic magmas at the Timber Mountain/Oasis Valley caldera complex, Nevada, *Geol. Soc. Am. Bull.*, 115 (5), 581-595, 2003.
- Bjarnason, I.T., W. Menke, O.G. Flovenz, and D. Caress, Tomographic Image of the Mid-Atlantic Plate Boundary in Southwestern Iceland, *Journal of Geophysical Research*, 98, 6607-6622, 1993.
- Blatter, D.L., I.S.E. Carmichael, A.L. Deino, and P.R. Renne, Neogene volcanism at the front of the central Mexican volcanic belt: Basaltic andesites to dacites with contemporaneous shoshonites and high TiO₂ lava, *Geol Soc Am Bull*, 113, 1324-1342, 2001.
- Bryan, S.E., A.E. Constantine, C.J. Stephens, A. Ewart, R.W. Schon, and J. Parianos, Early Cretaceous volcano-sedimentary successions along the eastern Australia continental margin: implications for the break-up of eastern Gondwana, *Earth Planet. Sci. Lett.*, 153, 85-102, 1997.

- Caress, D.W., M.K. McNutt, R.S. Detrick, and J.C. Mutter, Seismic imaging of hotspot-related crustal underplating beneath the Marquesas Islands, *Nature*, 373, 600-603, 1995.
- Carracedo, J.C., S.J. Day, P. Gravestock, and H. Guillou, Later stages of volcanic evolution of La Palma, Canary Islands: Rift evolution, giant landslides, and the genesis of the Caldera de Taburiente, *Geol. Soc. Am. Bull.*, 111 (5), 755-768, 1999.
- Carrier, D.L., and D.S. Chapman, Gravity and thermal models for the Twin Peaks silicic volcanic center, southwestern Utah, *J. Geophys. Res.*, 86, 10,287-10,302, 1981.
- Carslaw, H.S., and J.C. Jaeger, *Conduction of Heat in Solids*, 510 pp., Oxford Univ Press, London, 1959.
- Cary, S., J. Gardner, and H. Sigurdsson, The intensity and magnitude of Holocene plinian eruptions from Mount St. Helens Volcano, *J. Volc. Geotherm. Res.*, 66 (1-4), 185-202, 1995.
- Cawthorn, R.G., and F. Walraven, Emplacement and crystallization time for the Bushveld Complex, *J. Petrol.*, 39 (9), 1669-1687, 1998.
- Chesner, C.A., and W.I. Rose, Stratigraphy of the Toba Tuffs and the evolution of the Toba Caldera Complex, Sumatra, Indonesia, *Bull. Volcanol.*, 53, 343-356, 1991.
- Chevallier, L., Tectonic and structural evolution of Gough Volcano: a volcanological model, *J. Volc. Geotherm. Res.*, 33, 325-336, 1987.
- Chiarabba, C., A. Amato, and P.T. Delaney, Crustal structure, evolution, and volcanic unrest of the Alban Hills, Central Italy, *Bull. Volc.*, 59, 161-170, 1997.
- Christiansen, R.L., The Quaternary and Pliocene Yellowstone Plateau volcanic field of Wyoming, Idaho, and Montana, in *US Geol Survey Prof Paper 729*, pp. 1-146, 2001.
- Christiansen, R.L., and R.H.J. Blank, Volcanic Stratigraphy of the Quaternary Rhyolite Plateau in Yellowstone National Park, in *Geology of Yellowstone National Park*, 1972.
- Clawson, S.R., R.B. Smith, and H.M. Benz, P wave attenuation of the Yellowstone Caldera from three-dimensional inversion of spectral decay using explosion source seismic data, *J. Geophys. Res.*, 94, 7205-7222, 1989.
- Condit, C., L.S. Crumpler, J. Aubele, and W. Elston, Patterns of volcanism along the southern margin of the Colorado Plateau: The Springerville Field, *J. Geophys. Res.*, 94 (B6), doi: 10.1029/88JB04190, 1989.
- Courtillot, V.E., and P.R. Renne, On the ages of flood basalt events, *Comptes Rendus Geosci.*, 335, 113-140, 2003.
- Crecraft, H.R., W.P. Nash, and S.H. Evans, Late Cenozoic volcanism at Twin Peaks, Utah: geology and petrology, *J. Geophys. Res.*, 86, 10,303-10,320, 1981.
- Crisp, J.A., Rates of Magma Emplacement and Volcanic Output, *Journal of Volcanology and Geothermal Research*, 20, 177-211, 1984.
- Criss, R.E., E.B. Ekren, and R.F. Hardyman, Casto Ring Zone: A 4500-km² fossil hydrothermal system in the Challis Volcanic Field, central Idaho, *Geology*, 12, 331-334, 1984.
- Darbyshire, F.A., I.T. Bjarnason, R.S. White, and O.G. Flovenz, Crustal structure above the Iceland mantle plume imaged by the ICEMELT refraction profile, *Geophys. J. Int.*, 135, 1131-1149, 1998.

- Davidson, J.P., K.M. Ferguson, M.T. Colucci, and M.A. Dungan, The origin and evolution of magmas from the San Pedro Pellado volcanic complex, S. Chile; multicomponent sources and open system evolution, *Contr. Min. Pet.*, 100 (4), 429-445, 1988.
- Davis, J.M., and C.J. Hawkesworth, Geochemical and tectonic transitions in the evolution of the Mogollon-Datil Volcanic Field, New Mexico, USA, *Chem. Geol.*, 119, 31-53, 1995.
- de Bremond d'Ars, J., C. Jaupart, and R.S.J. Sparks, Distribution of volcanoes in active margins, *Journal of Geophysical Research, B, Solid Earth and Planets*, 100 (10), 20,421-20,432, 1995.
- Detrick, R.S., A.J. Harding, G.M. Kent, J.A. Orcutt, J.C. Mutter, and P. Buhl, Seismic Structure of the Southern East Pacific Rise, *Science*, 259, 499-503, 1993.
- Doell, R.R., G.B. Dalrymple, R.L. Smith, and R.A. Bailey, Paleomagnetism, potassium-argon ages, and geology of rhyolites and associated rocks of the Valles Caldera, New Mexico, in *Studies in Volcanology: Geol. Soc. Am. Memoir*, edited by R.R. Coats, R.L. Hay, and C.A. Anderson, pp. 211-248, 1968.
- Doucelance, R., S. Escrig, M. Moreira, C. Gariepy, and M. Kurz, Pb-Sr-He isotope and trace element geochemistry of the Cape Verde Archipelago, *Geochim. Cosmochim. Acta*, 67, 3717-3733, 2003.
- Doukas, M.P., Road Guide to Volcanic Deposits of Mount St. Helens and Vicinity, Washington, *U.S. Geol. Surv. Bull.*, 1859, pp.53, 1990.
- Druitt, T.H., L. Edwards, R.M. Mellors, D.M. Pyle, R.S.J. Sparks, M. Lanphere, M. Davies, and B. Barriero, *Santorini Volcano*, Geological Society, London, 1999.
- Duffield, W.A., C.R. Bacon, and G.B. Dalrymple, Late Cenozoic volcanism, geochronology, and structure of the Coso Range, Inyo County, California, *J. Geophys. Res.*, 85, doi: 10.1029/0JGREA0000850000B5002381000001, 1980.
- Duncan, R.A., Age distribution of volcanism along aseismic ridges in the eastern Indian Ocean, *Proc. ODP Sci. Results* (507-517), 1991.
- Dvorak, J.J., and D. Dzurisin, Variations in Magma Supply Rate at Kilauea Volcano, Hawaii, *Journal of Geophysical Research*, 98, 22,255-22,268, 1993.
- Erlich, E.N., and O.N. Volynets, Genral problems of petrology and acid volcanism, *Bull. Volc.*, 42, 175-185, 1979.
- Esser, R.P., P.R. Kyle, and W.C. McIntosh, 40Ar/39Ar dating of the eruptive history of Mount Erebus, Antarctica: volcano evolution, *Bull. Volcanol.*, 66, 671-686, 2004.
- Evans, S.H., H.R. Crecraft, and W.P. Nash, K/Ar ages of silicic volcanism in the Twin Peaks/Cove Creek Dome area, southwestern Utah, *Isochron/West*, 28, 21-24, 1980.
- Farmer, G.L., D.E. Broxton, R.G. Warren, and W. Pickthorn, Nd, Sr, and O isotopic variations in metaluminous ash-flow tuffs and related volcanic rocks at the Timber Mountains/Oasis Valley caldera complex, SW Nevada: implications for the origin and evolution of large-volume silicic magma bodies, *Contr. Min. Pet.*, 109, 53-68, 1991.
- Fedotov, S.A., Temperatures of entering magma, formation and dimensions of magma chambers of volcanoes, *Bull. Volcanol.*, 45 (4), 333-347, 1982.
- Fitton, J.G., and D. James, Basic volcanism associated with intraplate linear features, *Phil. Trans. R. Soc. Lond.*, 317, 253-266, 1986.

- Fowler, S.J., W.A. Bohrsen, and F.J. Spera, Magmatic evolution of the Skye Igneous Centre, Western Scotland: modelling of assimilation, recharge, and fractional crystallization, *J. Petrol.*, 45 (12), 2481-2505, 2004.
- Francis, P.W., and C.J. Hawkesworth, Late Cenozoic rates of magmatic activity in the Central Andes and their relationships to continental crust formation and thickening, *Journal of the Geological Society of London*, 151, Part 5, 845-854, 1994.
- Freundt, A.H., and H.-U. Schmincke, Eruption and emplacement of a basaltic welded ignimbrite during caldera formation on Gran Canaria, *Bull. Volc.*, 56, 640-659, 1995.
- Frey, F.A., M.F. Coffin, P.J. Wallace, D. Weis, X. Zhao, S.W. Wise, Jr., V. Wahnert, D.A.H. Teagle, P.J. Saccocia, D.N. Reusch, M.S. Pringle, K. Nicolaysen, C.R. Neal, R.D. Muller, C.L. Moore, J.J. Mahoney, L. Keszthelyi, H. Inokuchi, R.A. Duncan, H. Delius, J.E. Damuth, D. Damascenco, H. Coxall, M. Borre, F. Boehm, J. Barling, N. Arndt, and M. Antretter, Origin and evolution of a submarine large igneous province: the Kerguelen Plateau and Broken Ridge, southern Indian Ocean, *Earth Planet. Sci. Lett.*, 176, 73-89, 2000.
- Gallagher, K., and C. Hawkesworth, Mantle plumes, continental magmatism, and asymmetry in the South Atlantic, *Earth Planet. Sci. Lett.*, 123, 105-117, 1994.
- Gamble, J.A., R.C. Price, I.E.M. Smith, W.C. McIntosh, and N.W. Dunbar, ⁴⁰Ar/³⁹Ar geochronology of magmatic activity, magma flux, and hazards at Ruapehu Volcano, Taupo Volcanic Zone, New Zealand, *J. Volc. Geotherm. Res.*, 120, 271-287, 2003.
- Gamble, J.A., C.P. Wood, R.C. Price, I.E.M. Smith, R.B. Stewart, and T. Waight, A fifty year perspective of magmatic evolution on Ruapehu Volcano, New Zealand; verification of open system behaviour in an arc volcano, *Earth Planet. Sci. Lett.*, 170, 301-314, 1999.
- Gerlach, D.C., Eruption rates and isotopic systematics of ocean islands: further evidence for small-scale heterogeneity in the upper mantle, *Tectonophys.*, 172, 273-289, 1990.
- Greeley, R., and B.D. Schneid, Magma generation on Mars: Amounts, rates, and comparisons with Earth, Moon, and Venus, *Science*, 254, 996-998, 1991.
- Grevenmeyer, I., E.R. Flueh, C. Reichert, J. Bialas, D. Klaschen, and C. Kopp, Crustal architecture and deep structure of the Ninetyeast Ridge hotspot trail from active-source ocean bottom seismology, *Geophysical Journal International*, 144, 414-431, 2001.
- Guillou, H., J.C. Carracedo, and S.J. Day, Dating of the Upper Pleistocene-Holocene volcanic activity of La Palma using the unspiked K-Ar technique, *J. Volc. Geotherm. Res.*, 86, 137-149, 1998.
- Haederle, M., and M. Atherton, Shape and intrusion style of the Coastal Batholith, Peru, *Tectonophys.*, 345, 17-28, 2002.
- Hall, M.L., C. Robin, B. Beate, P. Mothes, and M. Monzier, Tungurahua Volcano, Ecuador: structure, eruptive history, and hazards, *J. Volc. Geotherm. Res.*, 91, 1-21, 1999.
- Hardee, H.C., Incipient magma chamber formation as a result of repetitive intrusions, *Bull. Volcanol.*, 45 (1), 41-49, 1982.

- Harding, A.J., G.M. Kent, and J.A. Orcutt, A multichannel seismic investigation of upper crustal structure at 9°N on the East Pacific Rise: Implications for crustal accretion, *J. Geophys. Res.*, *98*, 13925-13944, 1993.
- Harding, A.J., J.A. Orcutt, M.E. Kappus, E.E. Vera, J.C. Mutter, P. Buhl, R.S. Detrick, and T.M. Brocher, Structure of Young Oceanic Crust at 13 degrees N on the East Pacific Rise From Expanding Spread Profiles, *Journal of Geophysical Research*, *94*, 12,163-12,196, 1989.
- Harford, C.L., M.S. Pringle, R.S.J. Sparks, and S.R. Young, The volcanic evolution of Montserrat using 40Ar/39Ar geochronology, in *The eruption of Soufriere Hills Volcano, Montserrat, from 1995 to 1999*, edited by T.H. Druitt, and B.P. Kokelaar, pp. 93-113, The Geological Society, London, 2002.
- Hasenaka, T., Size, distribution, and magma output rate for shield volcanoes of the Michoacan-Guanajuato volcanic field, Central Mexico, *Journal of Volcanology and Geothermal Research*, *63*, 13-31, 1994.
- Hasenaka, T., and I.S.E. Carmichael, The cinder cones of Michoacan-Guanajuato, Central Mexico: Their age, volume, and distribution, and magma discharge rate, *J. Volc. Geotherm. Res.*, *25*, 105-124, 1985.
- Hawkesworth, C., R. George, S. Turner, and G. Zellmer, Time scales of magmatic processes, *Earth Planet. Sci. Lett.*, *218*, 1-16, 2004.
- Heiken, G., F. Goff, J. Gardner, and W. Baldrige, The Valles/Toledo Caldera Complex, Jemez Volcanic Field, New Mexico, *Ann. Rev. Earth and Planet. Sci.*, *18*, 27-53, 1990.
- Henry, C.D., M.J. Kunk, and W.C. McIntosh, 40Ar/39Ar chronology and volcanology of silicic volcanism in the Davis Mountains, Trans-Pecos Texas, *Geol. Soc. Am. Bull.*, *106*, 1359-1376, 1994.
- Hildreth, W., Volcanological perspectives on Long Valley, Mammoth Mountain, and Mono Craters: several contiguous but discrete systems, *J. Volc. Geotherm. Res.*, *136*, 169-198, 2004.
- Hildreth, W., and J. Fierstein, Recent eruptions of Mount Adams, Washington Cascades, USA, *Bulletin of Volcanology*, *58* (6), 472-490, 1997.
- Hildreth, W., J. Fierstein, and M. Lanphere, Eruptive history and geochronology of the Mount Baker volcanic field, Washington, *Geol. Soc. Am. Bull.*, *115* (6), 729-764, 2003a.
- Hildreth, W., T.L. Grove, and M. Dungan, Introduction to Special section on open magmatic systems, *J. Geophys. Res.*, *91*, 5887-5889, 1986.
- Hildreth, W., M. Lanphere, and J. Fierstein, Geochronology and eruptive history of the Katmai volcanic cluster, Alaska Peninsula, *Earth Planet. Sci. Lett.*, *214*, 93-114, 2003b.
- Hildreth, W., and M.A. Lanphere, Potassium-argon geochronology of a basalt-andesite-dacite arc system: The Mount Adams volcanic field, Cascade Range of southern Washington, *GSA Bulletin*, *106*, 1413-1429, 1994.
- Hirn, A., A. Necessian, M. Sapin, F. Ferrucci, and G. Wittlinger, Seismic heterogeneity of Mt Etna: structure and activity, *Geophys. J. Int.*, *105*, 139-153, 1991.
- Hobden, B.J., B.F. Houghton, J.P. Davidson, and S.P. Weaver, Small and short-lived magma batches at composite volcanoes: time windows at Tongariro volcano, New Zealand, *J. Geol. Soc. London*, *156*, 865-868, 1999.

- Hobden, B.J., B.F. Houghton, M. Lanphere, and I.A. Nairn, Growth of Tongariro volcanic complex: New evidence from K-Ar age determinations, *New Zealand Jour. Geol. and Geophys.*, 39 (1), 151-154, 1996.
- Hoernle, K., and H.-U. Schmincke, The role of partial melting in the 15 Ma geochemical evolution of Gran Canaria: A blob model for the Canary Hotspot, *J. Petrol.*, 34, 599-626, 1993.
- Hoernle, K., and H.-U. Schmincke, The petrology of the tholeiites through melilite nephelinites on Gran Canaria, Canary Islands: Crystal fractionation, accumulation, depths of melting, *J. Petrol.*, 34, 573-597, 1993.
- Hooff, E.E.E., R.S. Detrick, D.R. Toomey, J.A. Collins, and J. Lin, Crustal thickness and structure along three contrasting spreading segments of the Mid-Atlantic Ridge, 33.5°-35°N, *Journal of Geophysical Research*, 105, 8205-8226, 2000.
- Johnson, J.S., S.A. Gibson, R.N. Thompson, and G.M. Nowell, Volcanism in the Vitim volcanic field, Siberia: Geochemical evidence for a mantle plume beneath the Baikal Rift Zone, *J. Petrol.*, 46 (7), 1309-1344, 2005.
- Jourdan, F., G. Feraud, H. Bertand, A. Kampunzu, G. Tshoso, M. Watkeys, and B. LeGall, Karoo large igneous province: Brevity, origin, and relation to mass extinction questioned by new ⁴⁰Ar/³⁹Ar age data, *Geology*, 33, 745-748, 2005.
- Kamata, H., and T. Kobayashi, The eruptive rate and history of Kuju Volcano in Japan during the past 15,000 years, *Journal of Volcanology and Geothermal Research*, 76 (1-2), 163-171, 1997.
- Kaneoka, I., H. Mehnert, S. Zashu, and S. Kawachi, Pleistocene volcanic activities in the Fossa Magna region, central Japan: K-Ar studies of the Yatsugatake volcanic chain, *Geochem. J.*, 14, 249-257, 1980.
- Karson, J.A., Internal structure of oceanic lithosphere: A perspective from tectonic windows, in *Faulting and magmatism at mid-ocean ridges*, edited by P.T.D. W. R. Buck, J. A. Karson, Y. Lagabrielle, pp. 177-218, AGU, 1998.
- Karson, J.A., Geologic Structure of the Uppermost Oceanic Crust Created at Fast- to Intermediate-Rate Spreading Centers, *Annual Reviews of Earth and Planetary Science*, 30, 347-384, 2002.
- Kay, S.M., and R.W. Kay, Role of crystal cumulates and the oceanic crust in the formation of the lower crust of the Aleutian arc, *Geology*, 13, 461-464, 1985.
- Klein, F.W., Patterns of Historical Eruptions at Hawaiian Volcanoes, *J. Volc. Geotherm. Res.*, 12, 1-35, 1982.
- Koyama, M., and Y. Hayakawa, Syn- and post-caldera eruptive history of Izu Oshima Volcano based on tephra and loess stratigraphy, *J. Geogr.*, 105, 133-162, 1996.
- Kumagai, H., T. Ohminato, M. Nakano, M. Ooi, A. Kubo, H. Inoue, and J. Oikawa, Very-Long-Period Seismic Signals and Caldera Formation at Miyake Island, Japan, *Science*, 293, 687-690, 2001.
- Kuntz, M.A., D.E. Champion, E.C. Spiker, and R.H. Lefebvre, Contrasting magma types and steady-state, volume-predictable basaltic volcanism along the Great Rift, Idaho, *Geol Soc Am Bull*, 97, 579-594, 1986.
- Larsen, G., Holocene eruptions within the Katla volcanic system, South Iceland: characteristics and environmental impact, *Joekull*, 49, 1-28, 2000.

- Lewis-Kenedi, C.B., R.A. Lange, C.M. Hall, and H. Delgado-Granados, The eruptive history of Tequila volcanic field, western Mexico: ages, volumes, and relative proportions of lava types., *Bull. Volc.*, 67, 391-414, 2005.
- Lipman, P.W., The roots of ash-flow calderas in western North America: windows into the tops of granitic batholiths, *J. Geophys. Res.*, 89, 8801-8841, 1984.
- Lipman, P.W., Declining growth of Mauna Loa during the last 100,000 years; rates of lava accumulation vs. gravitational subsidence, in *Mauna Loa Revealed: structure, composition, history, and hazards*, edited by J.M. Rhodes, and J.P. Lockwood, pp. 45-80, American Geophysical Union, Wash. DC, 1995.
- Luhr, J.F., The geology and petrology of Volcan San Juan (Nayrit, Mexico) and the compositionally zoned Tepic Pumice, *J. Volc. Geotherm. Res.*, 95, 109-156, 2000.
- Luhr, J.F., and I.S.E. Carmichael, The Colima Volcanic Complex, Mexico, *Contributions to Mineralogy and Petrology*, 71, 343-372, 1980.
- Marsh, B.D., Magma Chambers, *Ann. Rev. Earth Planet. Sci.*, 17, 439-474, 1989.
- Martin, D.P., and W.I. Rose, Behavioral patterns of Fuego Volcano, Guatemala, *J. Volc. Geotherm. Res.*, 10, 67-81, 1981.
- Marzoli, A., E.M. Piccirillo, P.R. Renne, G. Belleini, M. Iacumin, J.B. Nyobe, and A.T. Tongwa, The Cameroon Line revisited: Petrogenesis of continental basaltic magmas from lithospheric and asthenospheric sources, *J. Petrol.*, 41, 87-109, 2000.
- Maud, J.G., D.C. Rex, A.P. Leroex, and D.L. Reid, Volcanism on Gough Island: A revised stratigraphy, *Geological Magazine*, 125 (2), 175-181, 1988.
- McConnell, V.S., C.K. Shearer, J.C. Eichelberger, M.J. Keskinen, P.W. Layer, and J.J. Papike, Rhyolite intrusions in the intracaldera Bishop Tuff, Long Valley Caldera, California, *Journal of Volcanology and Geothermal Research*, 67, 41-60, 1995.
- Menke, W., M. West, B. Brandsdottir, and D. Sparks, Compressional and Shear Velocity Structure of the Lithosphere in Northern Iceland, *Bulletin of the Seismological Society of America*, 88, 1561-1571, 1998.
- Mertes, H., and H.-U. Schmincke, Mafic postassic lavas fo the Quaternary West Eifel volcanic field, I. major and trace elements, *Contr. Min. Pet.*, 89, 330-345, 1985.
- Miller, D.S., and R.B. Smith, P and S velocity structure of the Yellowstone volcanic field from local earthquake and controlled-source tomography, *J. Geophys. Res.*, 104, 15,105-15,121, 1999.
- Mori, J., D. Eberhart-Phillips, and D.H. Harlow, Three-dimensional velocity structure at Mount Pinatubo: Resolving magma bodies, in *Fire and mud: eruptions and lahars of Mount Pinatubo, Philippines*, edited by C.G. Newhall, and R.S. Punongbayan, pp. 371-385, U.S. Geol. Surv., Seattle, 1996.
- Moyer, T.C., and S. Esperanca, Geochemical and isotopic variations in a bimodal magma system: the Kaiser Spring Volcanic Field, Arizona, *J. Geophys. Res.*, 94 (B6), 7841-7859, 1989.
- Mullineaux, D.R., Pre-1980 tephra-fall deposits erupted from Mount St. Helens, Washington, *USGS Professional Paper 1563*, 1996.
- Nakamura, K., Volcano-stratigraphic study of Oshima volcano, Izu, *Bull. Earthquake Res. Inst. Tokyo*, 42, 649-728, 1964.
- Neal, C.R., J.J. Mahoney, L. Kroenke, R.A. Duncan, and M.G. Petterson, The Ontong Java Plateau, in *Large igneous provinces; continental, oceanic, and planetary*

- flood volcanism*, edited by J.J. Mahoney, and M.F. Coffin, pp. 183-216, AGU, Washington DC, 1997.
- Nicolaysen, K., F.A. Frey, K.V. Hodges, D. Weis, and A. Giret, $^{40}\text{Ar}/^{39}\text{Ar}$ geochronology of flood basalts from the Kerguelen Archipelago, southern Indian Ocean: implications for Cenozoic eruption rates of the Kerguelen plume, *Earth Planet. Sci. Lett.*, *174*, 313-328, 2000.
- Nielsen, R.L., and M.A. Dungan, The petrology and geochemistry of Ocate volcanic field, north-central New Mexico, *Geol. Soc. Am. Bull.*, *96*, 296-312, 1985.
- Nielson, D.L., and B.S. Sibbett, Geology of Ascension Island, South Atlantic Ocean, *Geothermics*, *25* (4-5), 427-448, 1996.
- Oishi, M., and T. Suzuki, Tephrostratigraphy and eruptive history of the Younger Tephra Beds from the Yatsugatake Volcano, Central Japan, *Bull. Volc. Soc. Japan*, *49* (1), 1-12, 2004.
- Olson, P., Mechanics of flood basalt magmatism, in *Magmatic Systems*, edited by M.P. Ryan, pp. 1-18, Academic Press, New York, 1994.
- Oversby, V.M., and P.W. Gast, Isotopic composition of lead from oceanic islands, *J. Geophys. Res.*, *75*, 2097-2114, 1970.
- Pankhurst, R.J., P.T. Leat, P. Sruoga, C.W. Rapela, M. Marquez, B.C. Storey, and T.R. Riley, The Chon Aike Province of Patagonia and related rocks in West Antarctica: a large silicic igneous province, *J. Volc. Geotherm. Res.*, *81*, 113-136, 1998.
- Paris, R., H. Guillou, J.C. Carracedo, and F.J. Perez-Torrado, Volcanic and morphological evolution of La Gomera (Canary Islands), based on new K-Ar ages and magnetic stratigraphy: implications for ocean island evolution, *J. Geol. Soc. London*, *162*, 501-512, 2005.
- Patino, L.C., M.J. Carr, and M.D. Feigenson, Local and regional variations in Central American arc lavas controlled by variations in subducted sediment input, *Contributions to Mineralogy and Petrology*, *138*, 265-283, 2000.
- Perry, F.V., B.M. Crowe, G.A. Valentine, and L.M. Bowker, Volcanism Studies: Final Report for the Yucca Mountain Project, Los Alamos National Laboratory, Los Alamos, New Mexico, 1998.
- Petford, N., and K. Gallagher, Partial melting of mafic (amphibolitic) lower crust by periodic influx of basaltic magma, *Earth Planet. Sci. Lett.*, *193*, 483-499, 2001.
- Plesner, S., P.M. Holm, and J.R. Wilson, $^{40}\text{Ar}/^{39}\text{Ar}$ geochronology of Santo Antao, Cape Verde Islands, *J. Volc. Geotherm. Res.*, *120*, 103-121, 2002.
- Quane, S.L., M.O. Garcia, H. Guillou, and T.P. Hulsebosch, Magmatic history of the East Rift Zone of Kilauea Volcano, Hawaii based on drill core from SOH1, *J. Volc. Geotherm. Res.*, *102*, 319-338, 2000.
- Reid, M.R., Timescales of magma transfer and storage in the crust, in *Treatise on Geochemistry*, pp. 167-193, Elsevier Ltd, 2003.
- Reidel, S.P., T.L. Tolán, P.R. Hooper, M.H. Beeson, K.R. Fecht, R.D. Bentley, and J.L. Anderson, The Grande Ronde Basalt, Columbia River Basalt Group; Stratigraphic descriptions and correlations in Washington, Oregon, and Idaho, *Geol. Soc. Am. Special Paper*, *239*, 21-53, 1989.
- Renne, P.R., and A.R. Basu, Rapid eruption of the Siberian Traps flood basalts at the Permo-Triassic boundary, *Science*, *253* (5016), 176-179, 1991.

- Riehle, J.R., D.A. Champion, and M.A. Lanphere, Pyroclastic deposits of Mount Edgumbe Volcanic Field, Southeast Alaska, *J. Volc. Geotherm. Res.*, 53 (1-4), 117-143, 1992.
- Riisager, P., J. Riisager, N. Abrahamsen, and R. Waagstein, New paleomagnetic pole and magnetostratigraphy of Faroe Islands flood volcanics, North Atlantic Igneous Province, *201* (2), 261-276, 2002.
- Rubin, A.M., Propagation of Magma-Filled Cracks, *Ann. Rev. Earth and Planet. Sci.*, 23, 287-336, 1995.
- Schweitzer, J.K., C.J. Hatton, and S.A. De Waal, Link between the granitic and volcanic rocks of the Bushveld Complex, South Africa, *J. African Ear. Sci.*, 24 (12), 95-104, 1997.
- Shaw, H., Links Between magma-Tectonic Rate Balances, Plutonism, and Volcanism, *Journal of Geophysical Research*, 90, 11,275-11,288, 1985.
- Shaw, H.R., The Fracture Mechanisms of Magma Transport from the Mantle to the Surface, in *Physics of Magmatic Processes*, pp. 201-264, Princeton University Press, 1980.
- Shaw, H.R., E.D. Jackson, and K.E. Bargar, Volcanic Periodicity Along the Hawaiian-Emperor Chain, *American Journal of Science*, 280-A, 667-708, 1980.
- Sherrod, D.R., J.G. Smith, and L.J.P.p. Muffler, Quaternary extrusion rates of the Cascade Range, northwestern United States and southern British Columbia
Special section on Geological, geophysical, and tectonic setting of the Cascade Range, *Geological, geophysical, and tectonic setting of the Cascade Range*, 95 (12), 19,465-19,474, 1990.
- Singer, B., R. Thompson, M. Dungan, T. Feely, S. Nelson, J. Pickens, L. Brown, A. Wulff, J. Davidson, and J. Metzger, Volcanism and erosion during the past 930 k.y. at the Tartara-San Pedro complex, Chilean Andes, *Geol. Soc. Am. Bull.*, 109, 127-142, 1997.
- Singer, B.S., M. J.D., and F. C.D., Mid-Pleistocene lavas from the Segouam Island volcanic center, central Aleutian arc: closed-system fractional crystallization of a basalt to rhyodacite eruptive suite, *Contr. Min. Pet.*, 110, 87-112, 1992.
- Sinton, C.W., R.A. Duncan, B.C. Storey, J. Lewis, and J. Estrada, An oceanic flood basalt province within the Caribbean plate, *Earth Planet. Sci. Lett.*, 155, 221-235, 1998.
- Smith, R.L., Ash-flow magmatism, *Geol. Soc. Am. Special Paper*, 180, 5-27, 1979.
- Spera, F.J., Physical properties of magmas, in *Encyclopedia of Volcanoes*, edited by H. Sigurdsson, pp. 171-190, Academic Press, San Diego, 2000.
- Spera, F.J., D.A. Yuen, and S.J. Kirschvink, Thermal boundary layer convection in silicic magma chambers: Effects of temperature-dependent rheology and implications for thermogravitational chemical fractionation, *J. Geophys. Res.*, 87, 8755-8767, 1982.
- Staples, R.K., R.S. White, B. Brandsdottir, W. Menke, P.K.H. Maguire, and J.H. McBride, Faroe-Iceland Ridge Experiment
1. Crustal structure of northeastern Iceland, *Journal of Geophysical Research*, 102, 7849-7866, 1997.

- Stewart, K., S. Turner, S. Kelley, C. Hawkesworth, L. Kirstein, and M. Mantovani, 3-D, Ar-Ar geochronology in the Parana continental flood basalt province, *Earth Planet. Sci. Lett.*, 143, 95-109, 1996.
- Sutton, A.N., S. Blake, C.J.N. Wilson, and B.L. Charlier, Late Quaternary evolution of a hyperactive rhyolite magma system: Taupo volcanic centre, New Zealand, *Journ. Geophys. Soc. Lon.*, 157 (Part 3), 537-552, 2000.
- Svensen, H., S. Planke, A. Malthe-Sorensen, B. Jamtveit, R. Myklebust, T.R. Eidem, and S. Rey, Release of methane from a volcanic basin as a mechanism for initial Eocene global warming, *Nature*, 429, 542-545, 2004.
- Tanaka, K.L., E.M. Shoemaker, G.E. Ulrich, and E.W. Wolfe, Migration of volcanism in the San Francisco volcanic field, Arizona, *Geol. Soc. Am. Bull.*, 97 (2), 129-141, 1986.
- Tanguy, J.C., The storage and release of magma on Mount Etna: A discussion, *J. Volc. Geotherm. Res.*, 6, 179-188, 1979.
- Thouret, J.-C., A. Finizola, M. Fornari, A. Legeley-Padovani, J. Suni, and M. Frechen, Geology of El Misti volcano near the city of Arequipa, Peru, *Geol. Soc. Am. Bull.*, 113, 1593-1610, 2001.
- Togashi, S., N. Miyaji, and H. Yamazaki, Fractional Crystallization in a large tholeiitic magma chamber during the early stage of Younger Fuji Volcano, *Bull. Volc. Soc. Japan*, 36, 269-280, 1991.
- Tolan, T.L., S.P. Reidel, M.H. Beeson, J.L. Anderson, K.R. Fecht, and D.A. Swanson, Revisions to the estimates of the areal extent and volume of the Columbia River Basalt Group, *Geol. Soc. Am. Special Paper*, 239, 1-20, 1989.
- Tolstoy, M., A.J. Harding, and J.A. Orcutt, Crustal thickness on the Mid-Atlantic Ridge; bull's-eye gravity anomalies and focused accretion, *Science*, 262 (5134), 726-729, 1993.
- Trusdell, F.A., R.B. Moore, V. Carvalho-Martins, and A. Querido, The eruption of Fogo Volcano, Cape Verde Islands, April-May, 1995, *Eos. Trans. Am. Geophys. U.*, 76 (46 Fall Meet. Suppl.), 681, 1995.
- Tucholke, B., J. Lin, M. Kleinrock, M.A. Tivey, T. Reed, J. Goff, and G. Jaroslow, Segmentation and crustal structure of the western Mid-Atlantic Ridge flank, 25°25'-27°10'N and 0-29 m.y., *J. Geophys. Res.*, 102 (B5), 10,203-10,223, 1997.
- Twist, D., and B.M. French, Voluminous acid volcanism in the Busheveld Complex: A review of the Rooiberg Felsite, *Bull. Volc.*, 46, 225-242, 1983.
- Verhoogen, J., Petrological evidence on temperature distribution in the mantle of the earth, in *Symposium on the interior of the earth*, edited by W.H. Bucher, pp. 85-92, 1954.
- Vidal, V., and A. Bonneville, Variations of the Hawaiian hot spot activity revealed by variations in the magma production rate, *J. Geophys. Res.*, 109, 10.1029/2003JB002559, 2004.
- Wadge, G., The storage and release of magma on Mount Etna, *J. Volc. Geotherm. Res.*, 2, 361-384, 1977.
- Wadge, G., Output rate of magma from active central volcanoes, *Nature*, 288, 253-255, 1980.
- Wadge, G., Steady State Volcanism: Evidence from Eruption Histories of Polygenetic Volcanoes, *Journal of Geophysical Research*, 87, 4035-4049, 1982.

- Wadge, G., Comparison of volcanic production rates and subduction rates in the Lesser Antillies and Central America, *Geology*, 12, 555-558, 1984.
- Walker, G.P.L., Basaltic-volcano systems, *Magmatic Processes and Plate Tectonics, Geological Society Special Publication*, 76, 3-38, 1993.
- Weiland, C.M., L.K. Steck, P.B. Dawson, and V.A. Korneev, Nonlinear teleseismic tomography at Long Valley caldera, using three-dimensional minimum travel time ray tracing, *Journal of Geophysical Research*, 100, 20,379-20,390, 1995.
- Wolfe, E.W., and R.P. Hoblitt, Overview of the eruptions, in *Fire and mud: eruptions and lahars of Mount Pinatubo, Philippines*, edited by C.G. Newhall, and R.S. Punongbayan, pp. 3-20, U.S. Geol. Surv., Seattle, 1996.
- Zielinski, R.A., and F.A. Frey, Gough Island: Evaluation of a fractional crystallization model, *Contr. Min. Pet.*, 29, 242-254, 1970.

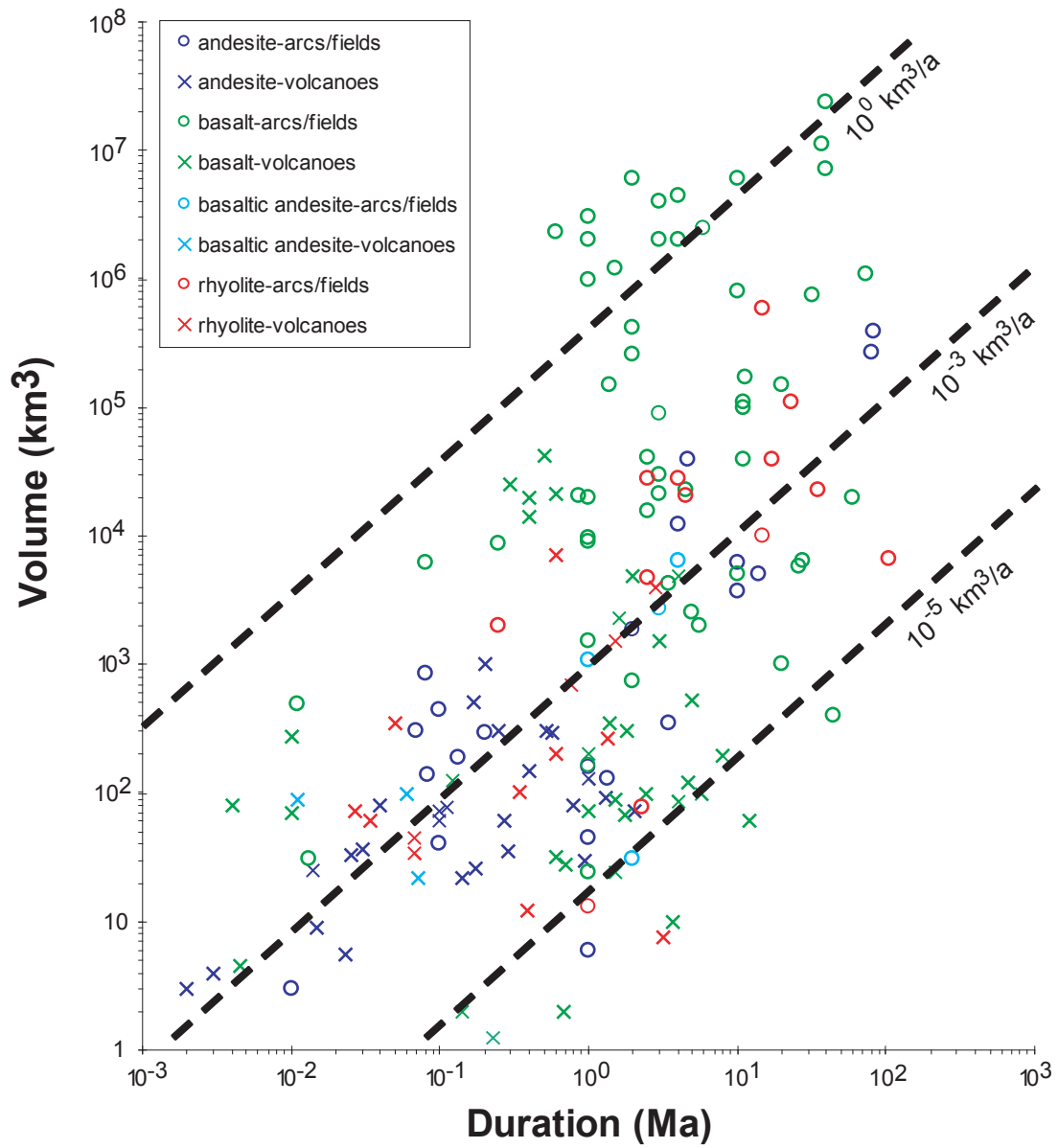


Figure 1

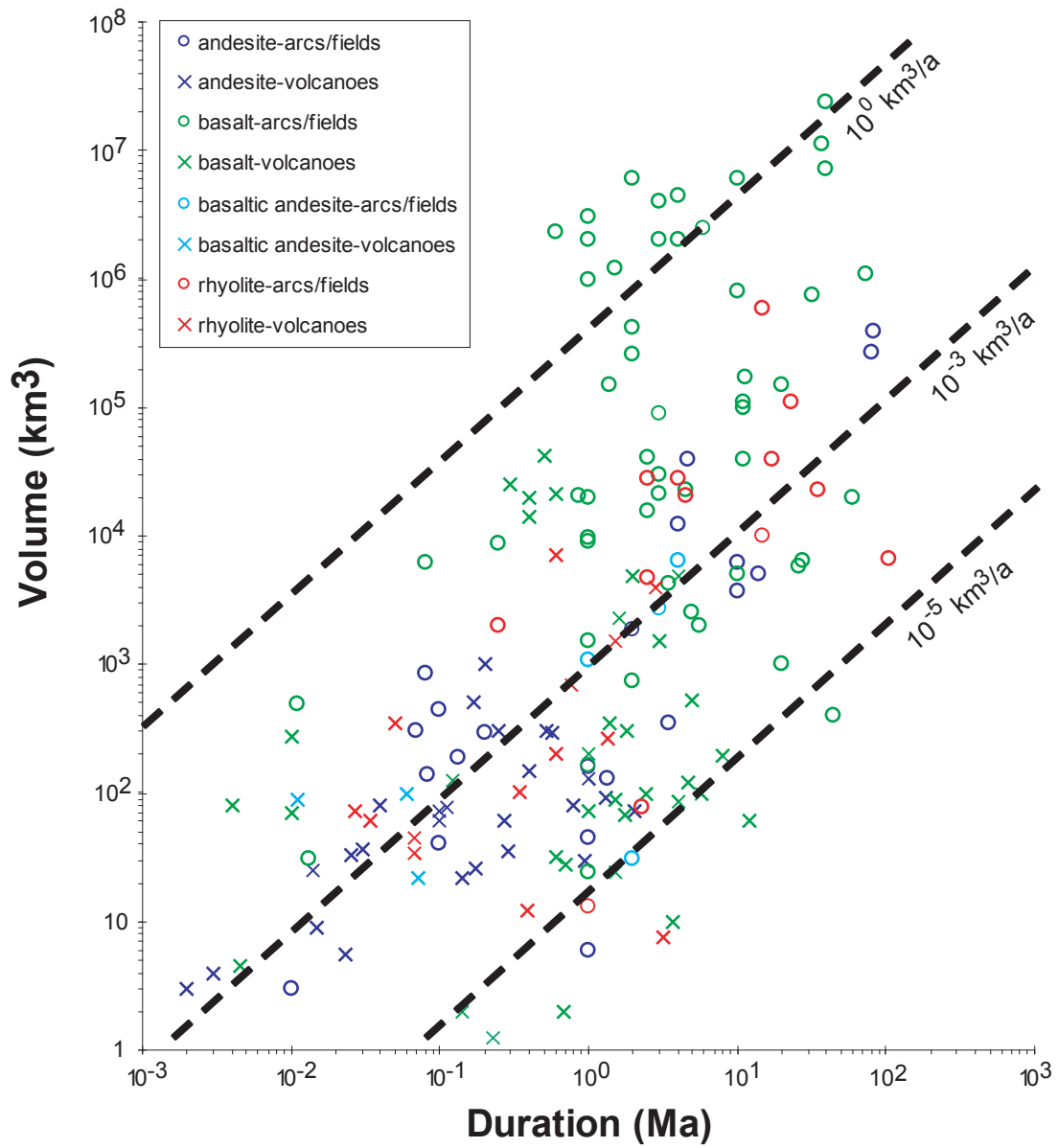


Figure 1

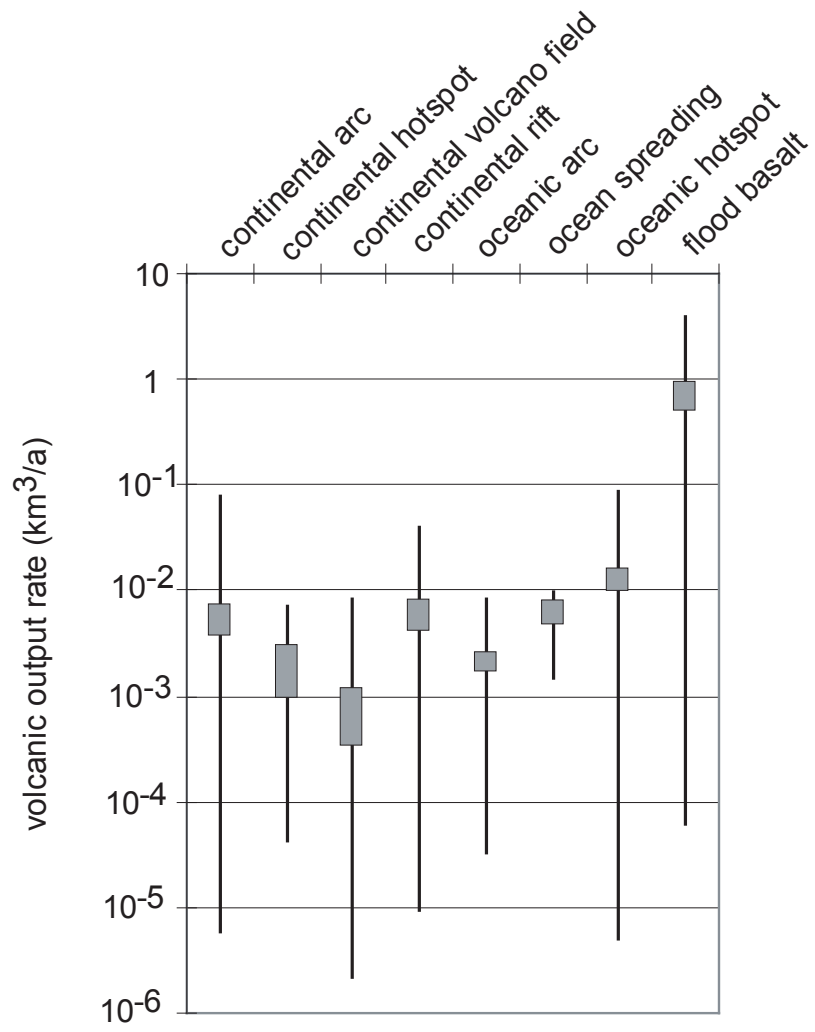


Figure 2

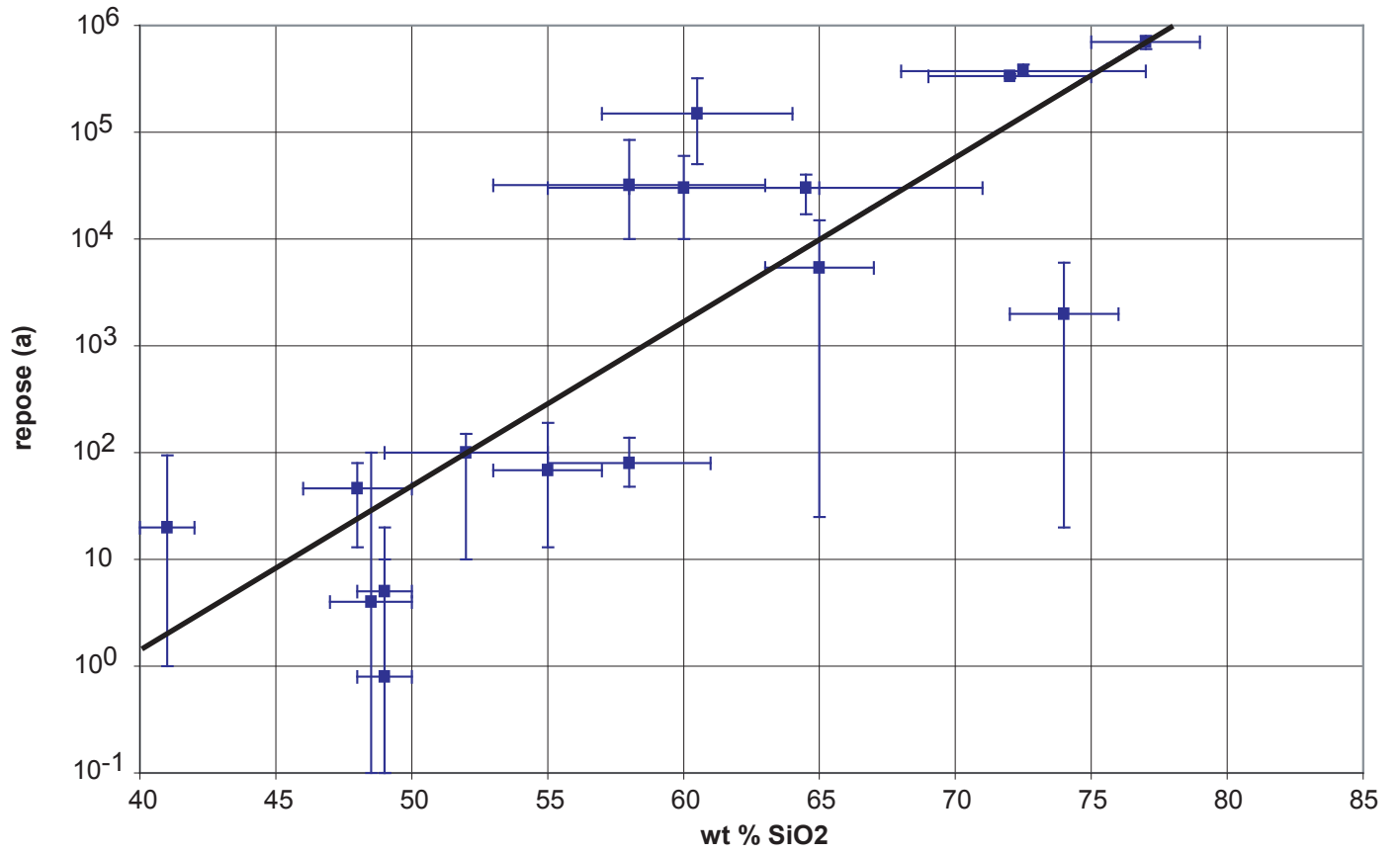


Figure 3

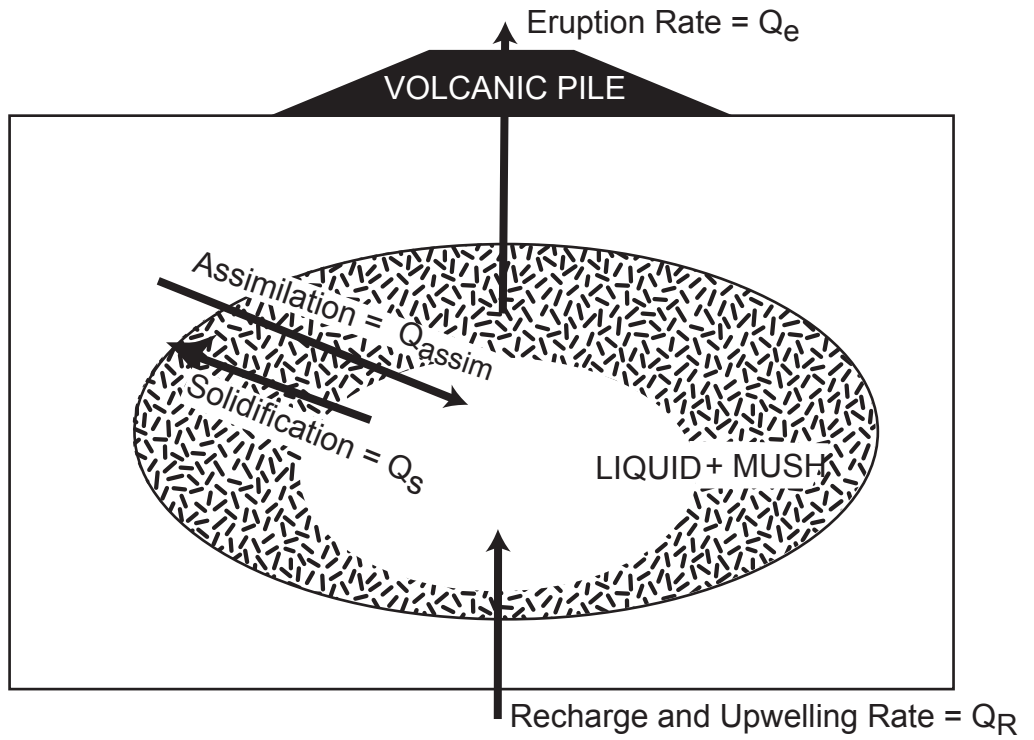
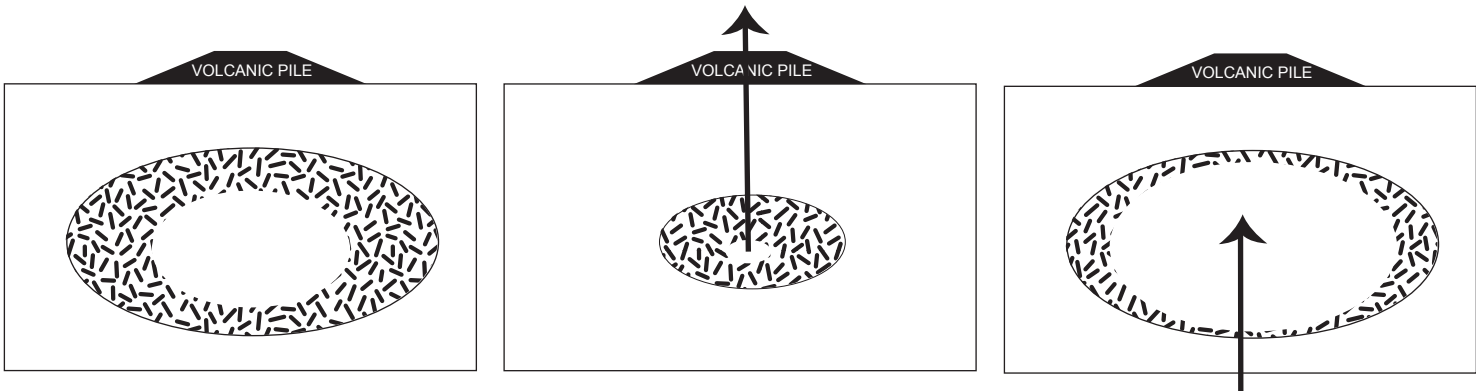


Figure 4

t₀: pre-existing magma

t₁: eruption

t₂: recharge



t₃: repose

t₄: eruption

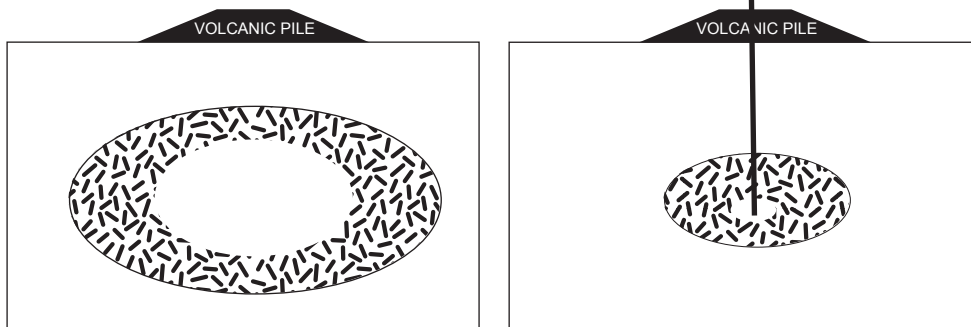


Figure 5

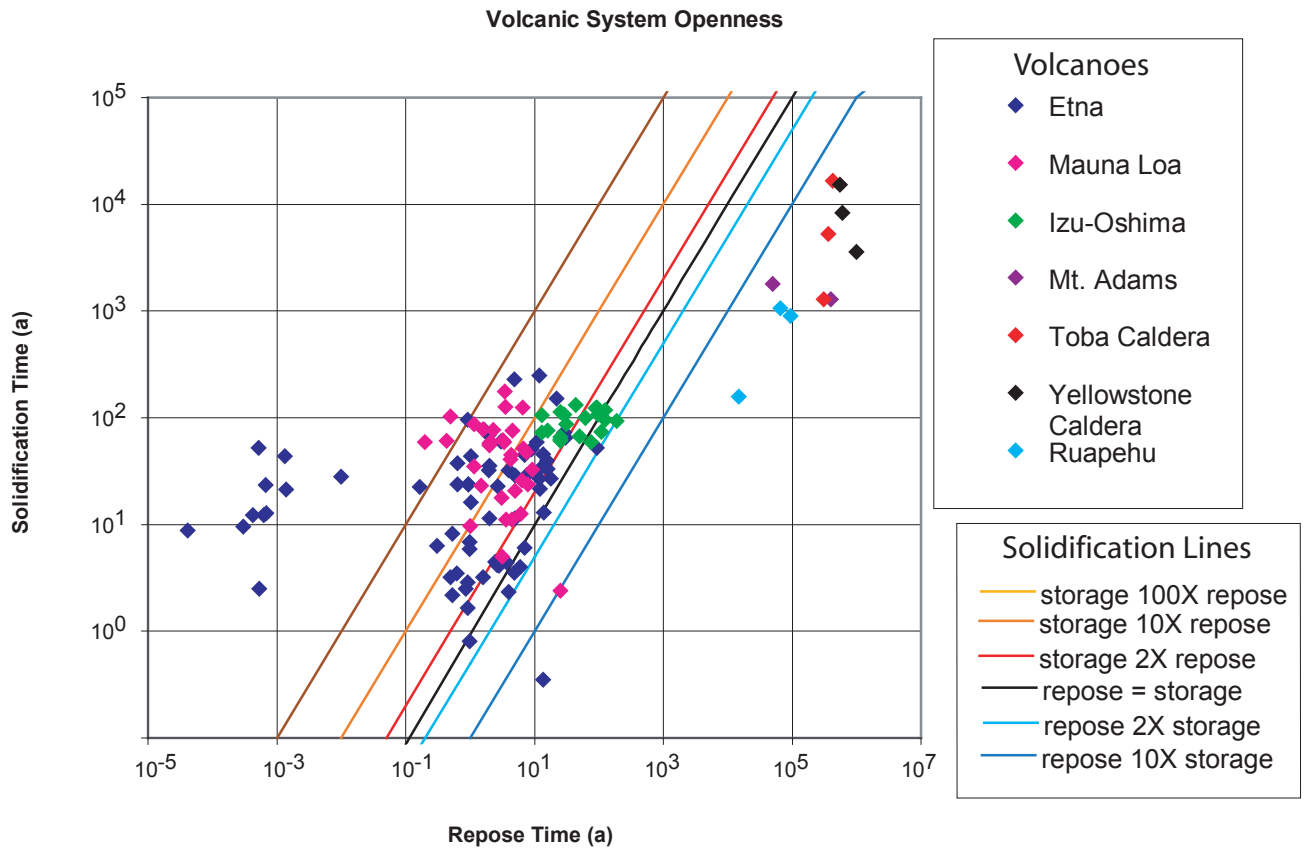


Figure 6